AD

CONTRACTOR REPORT ARCCB-CR-96025

A RAPID METHOD FOR DETERMINING STRESS CONCENTRATIONS FOR AUTOFRETTAGED TUBES CONTAINING MULTIPLE AXIAL PERFORATIONS WITHIN THE WALL

A. P. PARKER

ROYAL MILITARY COLLEGE OF SCIENCE
CRANFIELD UNIVERSITY, SWINDON, SN6 8LA, UK

AUGUST 1996

US ARMY ARMAMENT RESEARCH, DEVELOPMENT AND ENGINEERING CENTER
CLOSE COMBAT ARMAMENTS CENTER
BENÉT LABORATORIES
WATERVLIET, N.Y. 12189-4050

APPROVED FOR PUBLIC RELEASE; DISTRIBUTION UNLIMITED

DTIC QUALITY INSPECTED 3

19970108 032

DISCLAIMER

The findings in this report are not to be construed as an official Department of the Army position unless so designated by other authorized documents.

The use of trade name(s) and/or manufacturer(s) does not constitute an official indorsement or approval.

DESTRUCTION NOTICE

For classified documents, follow the procedures in DoD 5200.22-M, Industrial Security Manual, Section II-19 or DoD 5200.1-R, Information Security Program Regulation, Chapter IX.

For unclassified, limited documents, destroy by any method that will prevent disclosure of contents or reconstruction of the document.

For unclassified, unlimited documents, destroy when the report is no longer needed. Do not return it to the originator.

REPORT DOCUMENTATION PAGE

Form Approved
OMB No. 0704-0188

Public reporting burden for this collection of information is estimated to average 1 hour per response, including the time for reviewing instructions, searching existing data sources, gathering and maintaining the data needed, and completing and reviewing the collection of information. Send comments regarding this burden estimate or any other aspect of this collection of information, including suggestions for reducing this burden, to Washington Headquarters Services, Directorate for Information Operations and Reports, 1215 Jefferson Davis Highway, Suite 1204, Arlington, VA 22202-4302, and to the Office of Management and Budget, Paperwork Reduction Project (0704-0188), Washington, DC 20503.

1. AGENCY USE ONLY (*Leave blank*)	2. REPORT DATE	3. REPORT TYPE AND DATES COVERED
	August 1996	Final

4. TITLE AND SUBTITLE
A RAPID METHOD FOR DETERMINING STRESS CONCENTRATIONS FOR AUTOFRETTAGED TUBES CONTAINING MULTIPLE AXIAL PERFORATIONS WITHIN THE WALL

5. FUNDING NUMBERS
European Research Office
Contract 7922-AN-06(70-1S)

6. AUTHOR(S)
A.P. Parker

7. PERFORMING ORGANIZATION NAME(S) AND ADDRESS(ES)
Royal Military College of Science
Cranfield University
Swindon, SN6 8LA, UK

8. PERFORMING ORGANIZATION REPORT NUMBER

9. SPONSORING/MONITORING AGENCY NAME(S) AND ADDRESS(ES)
U.S. Army ARDEC
Benet Laboratories, AMSTA-AR-CCB-O
Watervliet, NY 12189-4050

10. SPONSORING/MONITORING AGENCY REPORT NUMBER
ARCCB-CR-96025

11. SUPPLEMENTARY NOTES
J.H. Underwood - Benet Laboratories Project Engineer

12a. DISTRIBUTION/AVAILABILITY STATEMENT
Approved for public release; distribution unlimited.

12b. DISTRIBUTION CODE

13. ABSTRACT (*Maximum 200 words*)

A simple method is developed for the determination of the stress concentration factor (SCF) arising from multiple, periodic, axial, elliptical holes within the wall of a gun tube. The model is based upon a simple superposition procedure with "capping" of any stresses that exceed yield magnitude, and is able to incorporate autofrettage residual stresses.

There are two potential failure locations, namely the bore (radius R_1) and the point on the hole boundary nearest the bore (radius R_H). By plotting the ratio of stress ranges due to firing at these two locations, taking account of pressure entering bore cracks, straightforward design plots of stress range ratio permit the selection of optimum radial hole location. This location is found to vary with the eccentricity of the hole's elliptical shape.

The choice of ideal ellipse eccentricity depends upon R_H, percentage overstrain, and ratio of firing pressure/yield strength. A near optimum value for the case $R_H/R_1 = 1.4$ is provided by the circular hole.

A straightforward design procedure is proposed which requires only standard compendia in order to optimize hole shape.

14. SUBJECT TERMS
Autofrettage, Fatigue Lifetimes, Axial Holes, Channels, Residual Stress, Stress Concentration, Thick Cylinders

15. NUMBER OF PAGES
26

16. PRICE CODE

17. SECURITY CLASSIFICATION OF REPORT	18. SECURITY CLASSIFICATION OF THIS PAGE	19. SECURITY CLASSIFICATION OF ABSTRACT	20. LIMITATION OF ABSTRACT
UNCLASSIFIED	UNCLASSIFIED	UNCLASSIFIED	UL

TABLE OF CONTENTS

Page

ILLUSTRATIONS

DTIC QUALITY INSPECTED 3

A Rapid Method for Determining Stress Concentrations for Autofrettaged Tubes Containing Multiple Axial Perforations Within the Wall

A P Parker

INTRODUCTION

The use of autofrettage to enhance fatigue lifetimes of thick cylinders subjected to internal cyclic pressurization is well known and relatively well understood. Recent work has addressed the problems associated with geometrical changes which remove the initial axi-symmetric nature of geometry and stressing of these tubes, namely:

a. Axial erosion grooves, *which arise after autofrettage,* along the bore of the cylinder, Ref 1.
b. Cross-bore holes normal to the tube axis (Ref 2) and inclined at an angle to the axis (Ref 3). These holes likewise are *introduced after autofrettage.*

The purpose of the work presented herein is to analyze, using elastic and simplified elastic/plastic stress analysis methods, the fatigue behaviour of cylinders which contain a series of equally-spaced holes orientated parallel to the tube axis and *which were introduced prior to autofrettage.* The cross-sectional shape of these holes may be somewhat arbitrary, but is shown diagramatically in Figure 1 as circular.

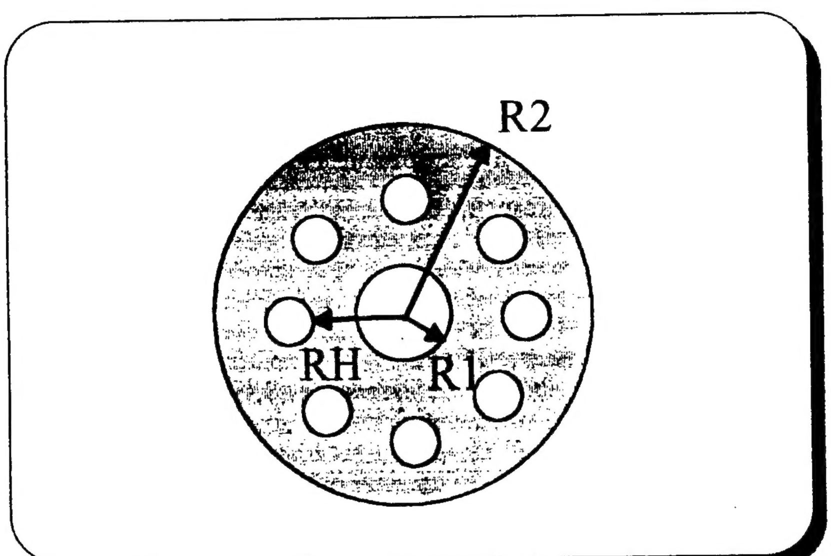

Figure 1

MODEL

The model is summarised below (refer to Figure 1).

a. Tube radius ratio R2/R1 = 2.0 and 1.8
b. One or 24 arbitrarily shaped cooling holes with critical locations at radius RH
c. Cooling hole size small relative to tube radii
d. Cooling hole size significant relative to hole spacing (multiple cooling holes)
e. Tresca yield criterion applies. If stress at any location exceeds yield, whether in tension or compression, loading or unloading, it is capped at yield magnitude
f. The following variables and associated ranges were examined:

$$1.0 \leq R_H/R_1 \leq R_2/R_1$$

$$K_T^{(1)} = 1.5, 2.0, 2.5, 3.0, 3.5, 4.0$$

where $K_T^{(1)}$ is conventional stress concentration factor (uniaxial tension)

$$\%Autofrettage = 0, 30, 40, 50, 60, 70, 80, 90, 100$$

$$Firing\ Pressure\ (p^f) = 33\%\ and\ 40\%\ of\ Yield\ Strength$$

ASSUMED HISTORY

Zero interference fit between inner and outer tube ('neat fit')

Case 1 : No autofrettage, possible yielding at hole during first firing (capped at yield magnitude) followed by elastic unloading

Case 2 : Autofrettage, yielding at hole during loading (capped at yield magnitude in tension) and possibly during removal of autofrettage pressure (again, capped at yield magnitude in compression).

Assume 70% of 'ideal' autofrettage field locked in at bore (this encompasses Bauschinger effect)

ELASTIC BIAXIAL STRESS FIELD EFFECTS

Radial (σ_r) and Hoop (σ_θ) stresses generated by the application of internal pressure are perceived by the hole(s) as a biaxial stress field. It is important to understand the stress concentration effects around a circular or elliptical cut-out in a biaxial stress field.. This is illustrated in Figure 2 for the case of a single elliptical cut-out having major axis *2a* and minor axis *2b* with principal stresses σ_1 and σ_2 applied normal to the axes of the ellipse. We note later that σ_1 and σ_2 are analogous to σ_θ and σ_r respectively.

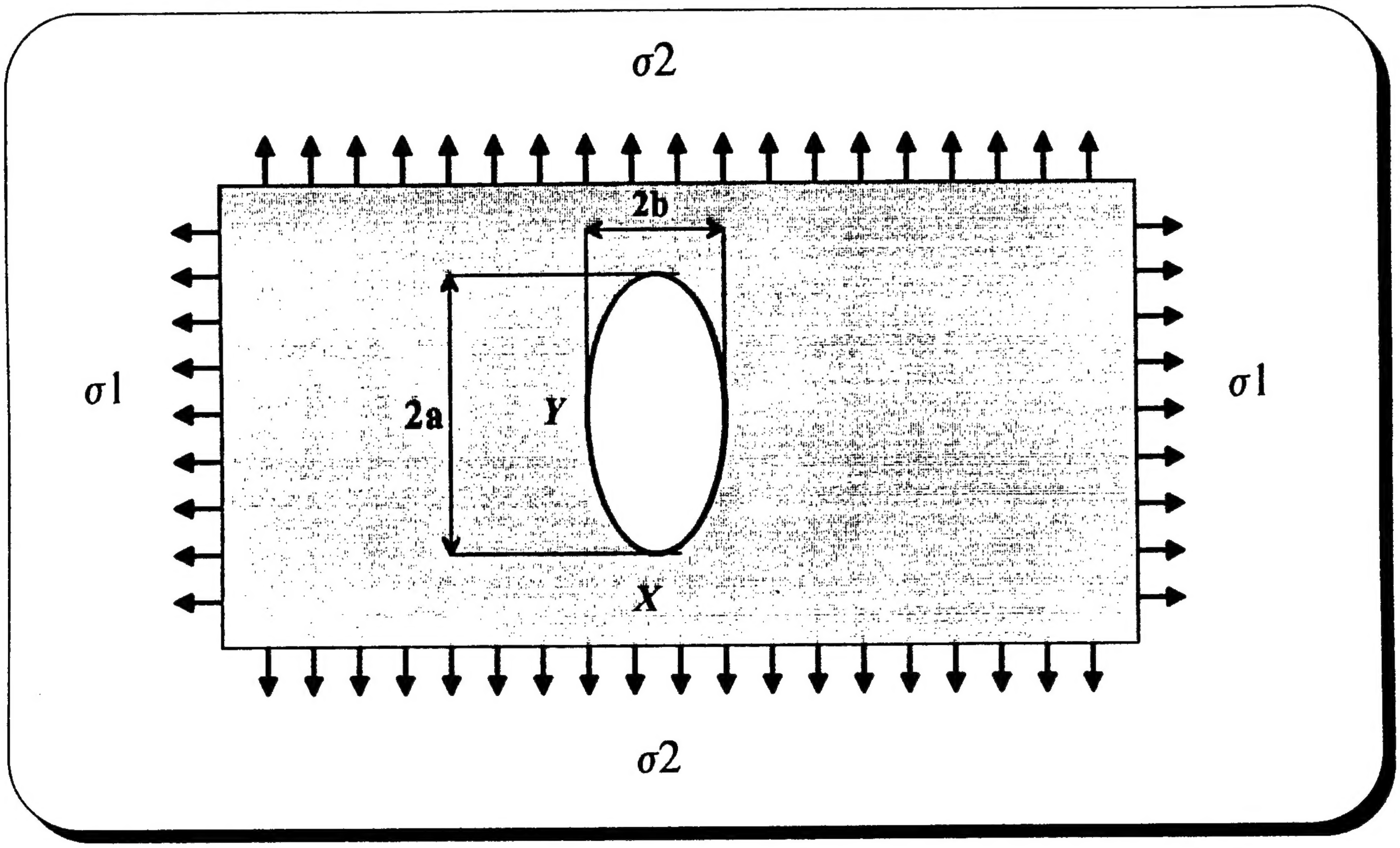

Figure 2

The Maximum Principal Stress at point X is given by:

$$\alpha\left[1 + 2\left(\frac{a}{b}\right)\right]\sigma_1 - \beta\delta\sigma_1 \qquad (1)$$

where $$\delta = \frac{\sigma_2}{\sigma_1}$$

and we designate $$K_T^{(1)} = \alpha\left[1 + 2\left(\frac{a}{b}\right)\right] \qquad (2)$$

and $$K_T^{(2)} = -\beta\delta \qquad (3)$$

and for later use $$K_T^{(T)} = K_T^{(1)} + K_T^{(2)} \qquad (4)$$

where, for a single hole $\alpha = \beta = 1$.

For the case a = b, $\sigma_2 = 0$ this reduces to the familiar stress concentration factor for a circular hole, of value +3.

Now consider the effect of creating an infinite array of such holes (Figure 3), with spacing of 2d between centers. There is then a rearrangement of the stress patterns and a modification of the stress concentration factor in that α and β are liable to change.

Turning first to β, the value of unity is the analytic solution for :

- A single ellipse (including the special case of a circle)
- An infinite array of cracks (i.e. a = 0, all physically acceptable values of d)

it is therefore inferred that the value of β = unity applies to the case of a single ellipse and to an array of ellipses. In any case, as will be demonstrated later, the magnitude of the hoop stresses is much greater than the radial stresses and therefore any errors in β will be relatively insignificant.

It is possible to obtain values of α from a compendium of stress concentration factors due to Peterson (1974), Ref 4. The relevant results presented therein summarise the work of Nisitani (1968), Ref 5 and Schulz (1942, 1943-1945), Ref 6. Unfortunately the results are only presented for the case $a \geq b$, which includes the case of the circle. These results are also further restricted to 0 <= a/d <= 0.75 (for a = b) and 0 <= a/d <= 0.5 (for a > b).

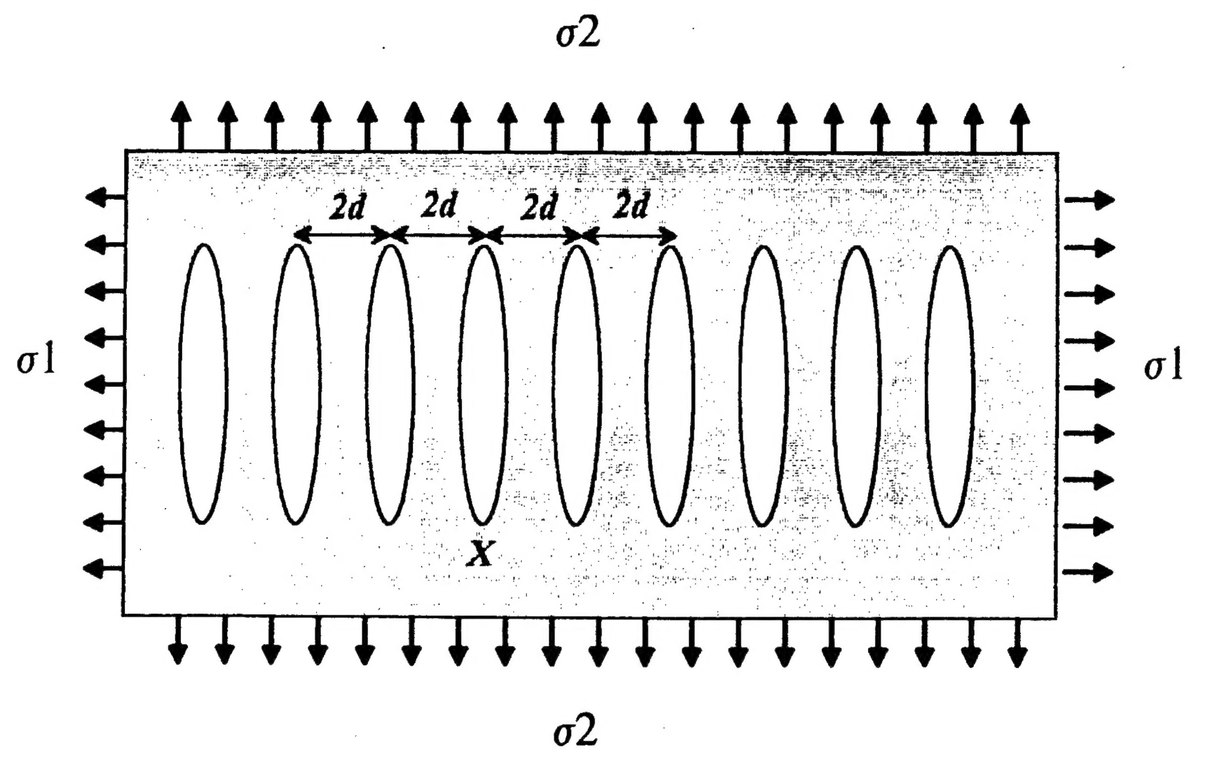

Figure 3

Turning to the particular case of an array of 24 circular holes (a = b) conforming with the general geometry shown in Figure 4 we find that a/d = b/d = 0.425, giving (from Peterson) a value $\alpha = 0.76$ (note this figure can be obtained from Peterson, Fig 113, Fig 134 or Fig 135). Hence the single circular hole uniaxial SCF value ($K_T^{(1)}$) of +3 is reduced to 2.28, whilst β remains at unity. Values of α for the circular hole and $0 <= a/d <= 0.75$ are reproduced as Figure 5 directly from Peterson (Fig 113).

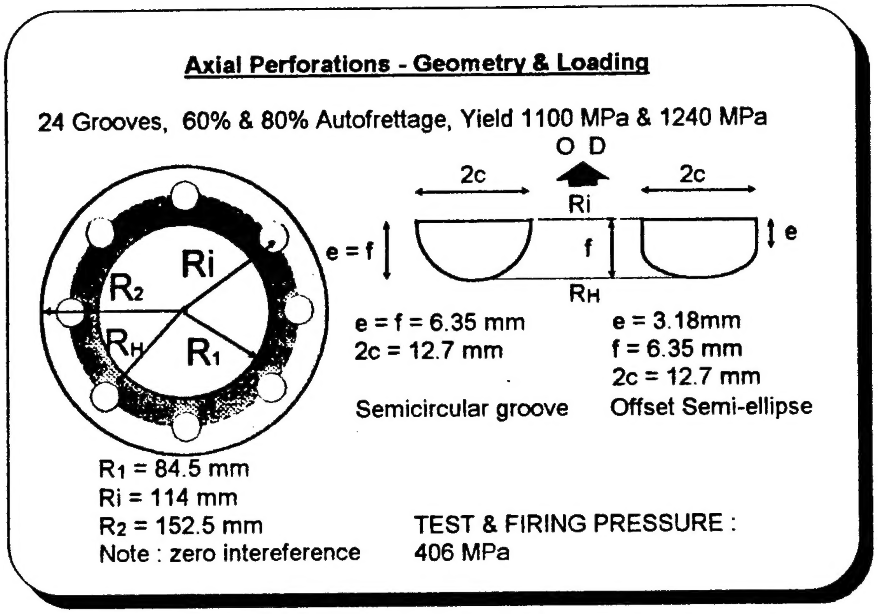

Figure 4

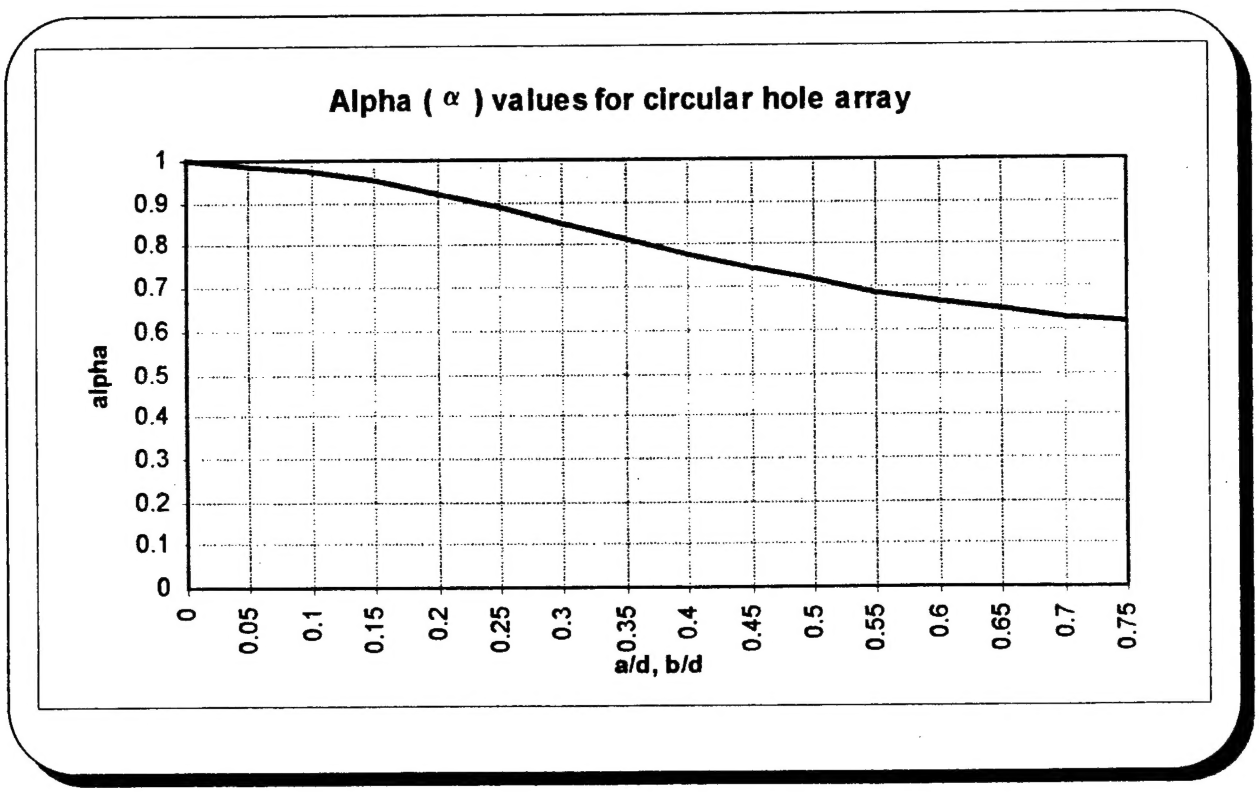

Figure 5

Now maintaining a b/d ratio of 0.425 and allowing a/b to vary we find that when

a/b = 2	we obtain	a/d = 0.85
a/b = 0.5	we obtain	a/d = 0.2125

Using Peterson, Fig 134, we find that for the case a/b = 2, using a/d = 0.85, a value α = 0.69 is extrapolated; this gives a uniaxial SCF of (0.69x(1+2x(a/b))) or 3.45. Whilst data are not presented for the case *a* < *b* it is possible to infer some approximate values using Peterson, Fig 134. On this basis, using a/d = 0.2125, a value α = 0.87 is obtained for a/b = 0.5, this gives a uniaxial SCF of (0.87x(1+2x(a/b))) or 1.74. The inference is clear: whilst the 'shielding' effect does reduce SCF proportionately more with increasing a/b, this effect is not sufficient to prevent the significant increase of SCF with increasing a/b ratio.

At this point we note that σ_1 and σ_2 are analogous to σ_θ and σ_r respectively, and that since the latter are of opposite sign as a result of internal pressure, the existence of the minus sign in Equation (1) means that the effects on the total SCF ($K_T^{(T)}$) are additive.

RESULTS

The results are presented in dimensionless form. Since a major objective is likely to be to optimise the design to produce similar <u>positive</u> cyclic stress ranges at both bore ($\Delta\sigma^B$) and hole ($\Delta\sigma^H$) the main parameter considered is the ratio $\Delta\sigma^H/\Delta\sigma^B$, designated RΔ. This ratio is presented numerically and graphically in Appendix A. (Note: this approach is described at length in Reference 7)

NOTE THAT THE ABBREVIATION cSCF USED ON ALL PLOTS INDICATES <u>CONVENTIONAL</u> STRESS CONCENTRATION FACTOR, i.e. $K_T^{(1)}$ IN THE DEFINITIONS USED HEREIN. IN ALL CASES THE CURVES IMPLICITLY TAKE ACCOUNT OF THE CONTRIBUTION FROM RADIAL STRESSES AT THE GIVEN RADIAL LOCATION.

Case 1 - R2/R1 = 2.0

Pages A1 - A9 show the RΔ ratio ($\Delta\sigma^H/\Delta\sigma^B$) for a non-autofrettaged tube and for tubes with various percentage overstrains. The results for 60% autofrettage are shown further enlarged by restricting to 1.2<RH/R1<R2/R1 and also plotted as SCF versus RΔ ratio which permits the easy location of minima for any value of RH/R1.

Case 2 - R2/R1 = 1.8

Pages A10 - A17 show the RΔ ratio for tubes with various percentage overstrains. The results for 60% autofrettage are shown further enlarged by restricting to 1.2<RH/R1<R2/R1 and also plotted as SCF versus RΔ ratio which permits the easy location of minima for any value of RH/R1.

COMMENTARY

Referring to Appendix A we note some interesting features.

a. The choice of ideal $K_T^{(1)}$ depends upon RH/R1, percentage overstrain and ratio of Firing pressure/Yield strength

b. For the case RH/R1 = 1.4 the single circular hole ($K_T^{(1)} = 3$) produces a near optimum value.

c. For the case RH/R1 = 1.4, reducing $K_T^{(1)}$ below 3.0 invariably results in a detrimental increase in RΔ

d. In order to determine the optimum groove shape using only standard stress concentration manuals the following steps are necessary:

- Identify minimum RΔ and associated $K_T^{(1)}$ for relevant R2/R1 and RH/R1
- Using Peterson calculate value of α for number of holes and hole size
- Use SCF and α in Equation (1) to determine optimum ellipse eccentricity

It is important to note that the above approach can also be applied to arbitrary groove shapes by undertaking a straightforward, two-dimensional, numerical elastic stress analysis. In this case the arbitrary groove shape is modelled using (say) FE or BE methods, Figure 6, with internal pressure applied to the bore and $u_\theta = \tau_{r\theta} = 0$ along radii of symmetry. The value of $K_T^{(T)}$ being extracted for the critical point on the hole boundary. This requires a set of design curves based upon $K_T^{(T)}$ rather than $K_T^{(1)}$.

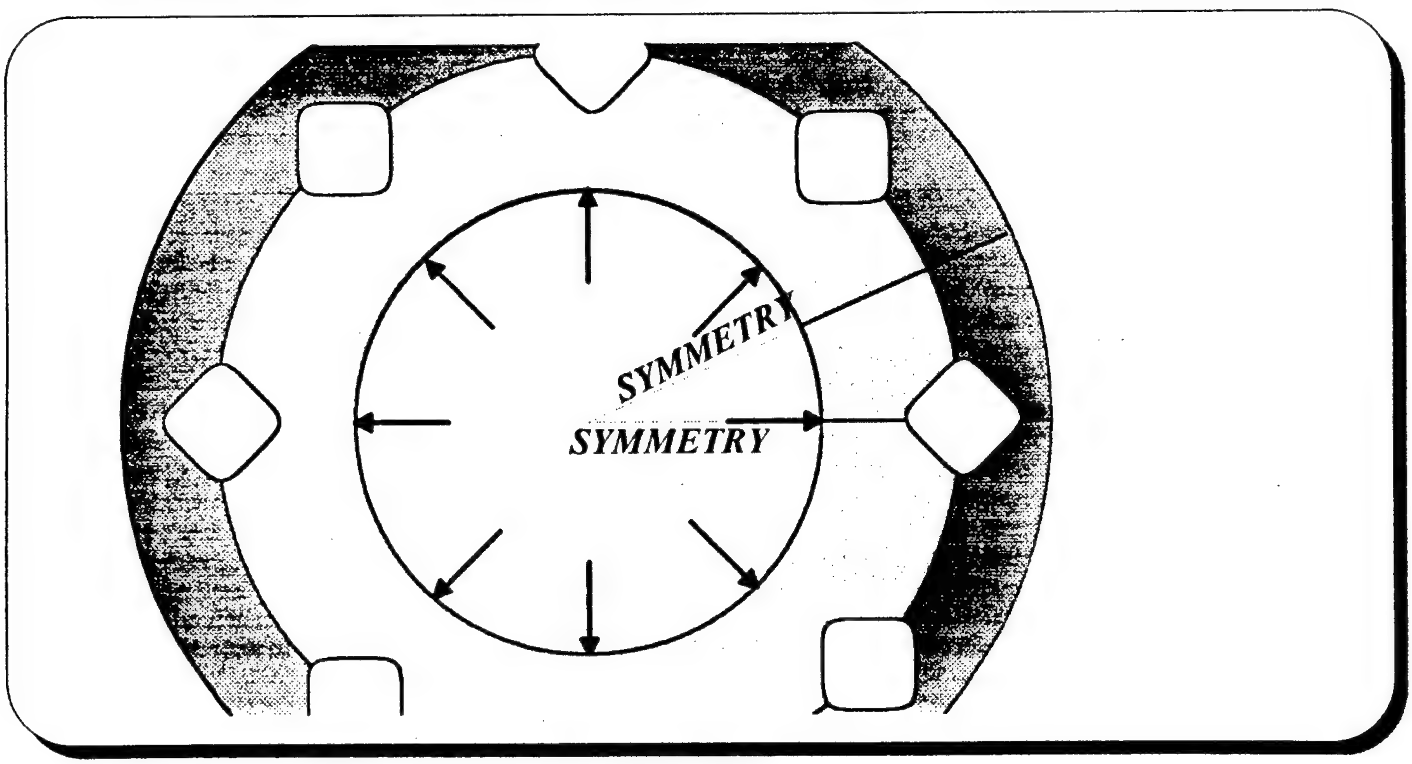

Figure 6

REFERENCES

1. Underwood, J H, and Parker, A P, *Fatigue Life Analysis and Tests for Thick-Walled Cylinders Including Effects of Overstrain and Axial Grooves,* PVP-Vol 280, Fatigue, Flaw Evaluation and Leak-Before-Break Assessments, ASME PVP Conference Proceedings, pp303-311, Minneapolis, 1994 . Published in Trans ASME PVP Journal, Vol 117, pp222-226 (1995)

2. Parker, A P and Underwood, J H, *Stress Concentration, Stress Intensity and Fatigue Crack Growth Along Evacuators of Pressurized, Autofrettaged Tubes,* ASME PVP Conference Proceedings, Hawaii, 1995 (In Press)(Accepted for publication in ASME PVP Journal, 1995)

3. Endersby, S, Bond, T and Parker A P, *Stress Concentration, Stress Intensity and Fatigue Crack Growth Along Angled Evacuators of Pressurized, Autofrettaged Tubes,* (In preparation for publication, 1995)

4. Peterson, R E, *Stress Concentration Factors*, Wiley (1974)

5. Nisitani, H, *Method of Approximate Calculation for Interference of Notch Effect and its Application,* Bull Japan Soc Mech Eng, 11, p725 (1968)

6. Schulz, K J, *On the State of Stress in Perforated Strips and Plates,* Proc Koninklyke Nederlandsche Akadamie van Wetenschappen (Netherlands Royal Academy of Science), Amsterdam, (6 papers) Vol 45, pp233, 341, 457, 524 (1942) Vol 46-48, pp 282, 292 (1943-45)

7. Parker, A P, Underwood, J H, *Some Methods of Representing Fatigue Lifetime as a Function of Stress Range and Initial Crack Length*, To be presented at ASTM National Fracture Symposium, Saratoga Springs, NY June 1996 and published in ASTM STP American Society for Testing and Materials. Philadelphia, (1996)

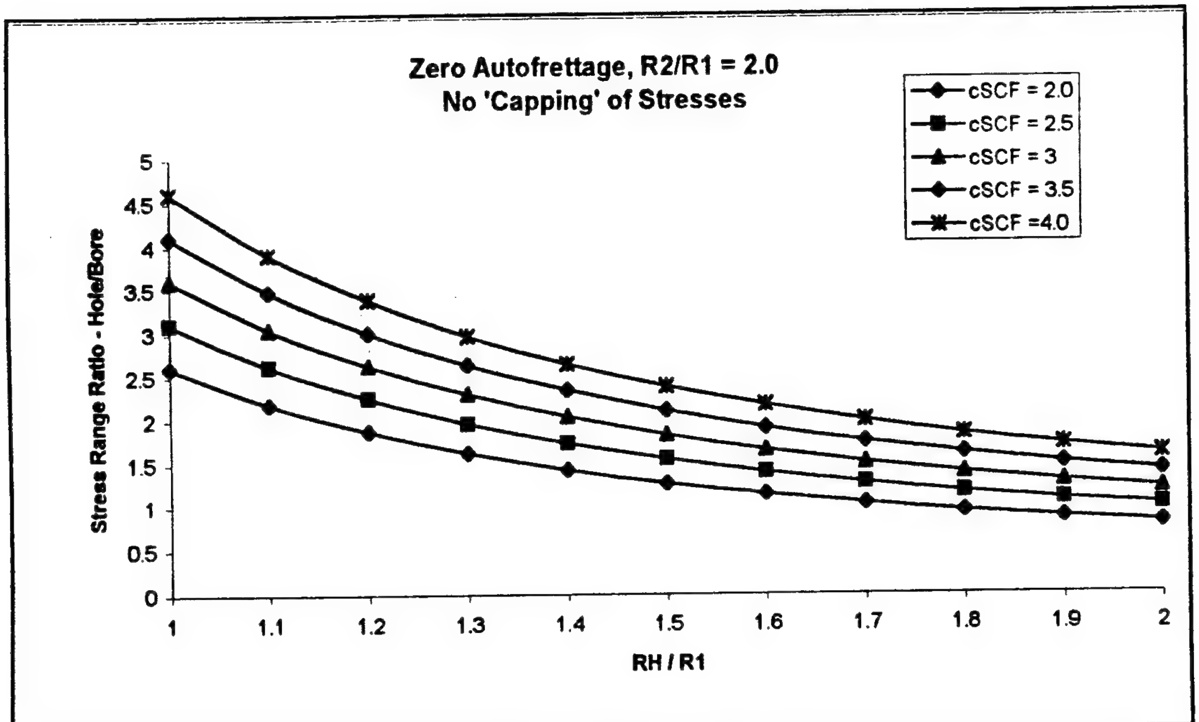
Zero Autofrettage, R2/R1 = 2.0
No 'Capping' of Stresses
cSCF = 2.0
cSCF = 2.5
cSCF = 3
cSCF = 3.5
cSCF =4.0
Stress Range Ratio - Hole/Bore
RH / R1
0
0.5
1
1.5
2
2.5
3
3.5
4
4.5
5
1
1.1
1.2
1.3
1.4
1.5
1.6
1.7
1.8
1.9
2

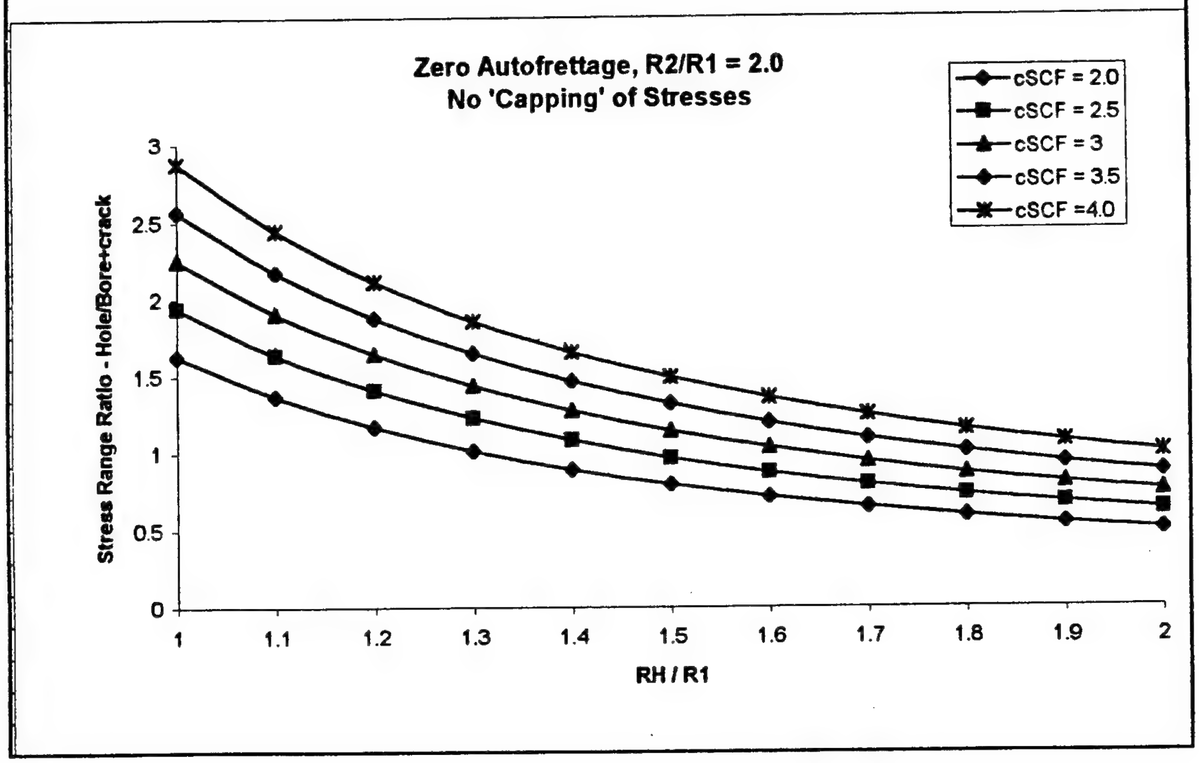
Zero Autofrettage, R2/R1 = 2.0
No 'Capping' of Stresses
cSCF = 2.0
cSCF = 2.5
cSCF = 3
cSCF = 3.5
cSCF =4.0
Stress Range Ratio - Hole/Bore+crack
RH / R1
0
0.5
1
1.5
2
2.5
3
1
1.1
1.2
1.3
1.4
1.5
1.6
1.7
1.8
1.9
2

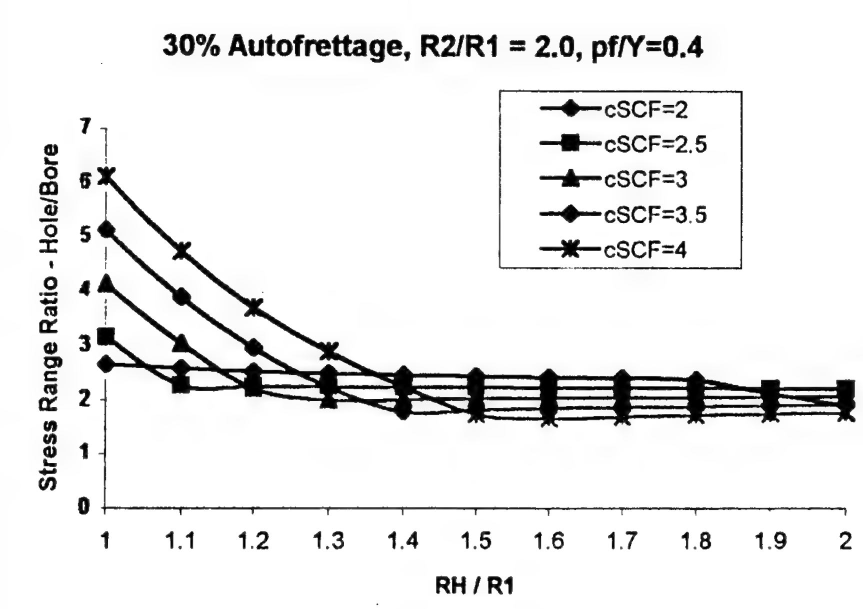
30% Autofrettage, R2/R1 = 2.0, pf/Y=0.4
cSCF=2
cSCF=2.5
cSCF=3
cSCF=3.5
cSCF=4
Stress Range Ratio - Hole/Bore
RH / R1

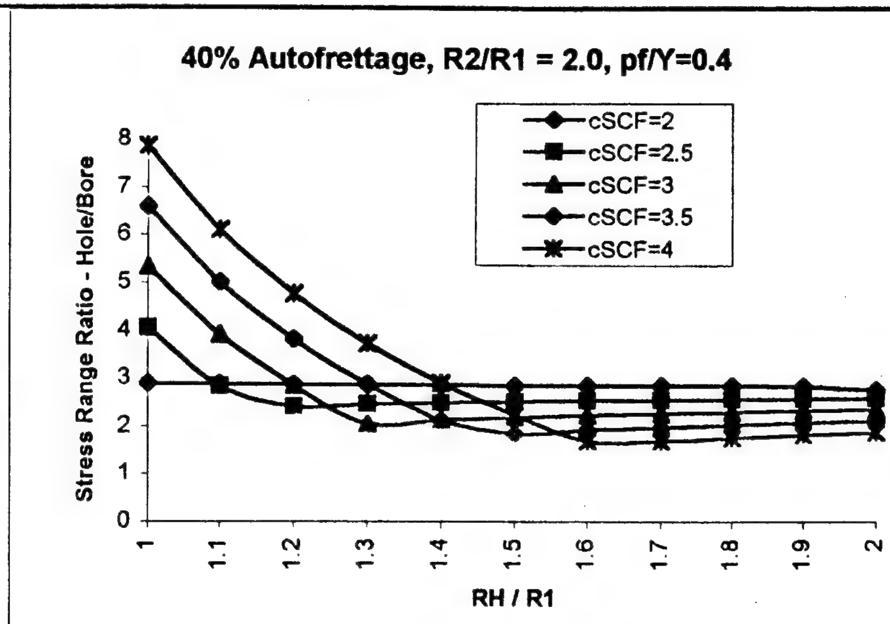
40% Autofrettage, R2/R1 = 2.0, pf/Y=0.4
cSCF=2
cSCF=2.5
cSCF=3
cSCF=3.5
cSCF=4
Stress Range Ratio - Hole/Bore
RH / R1

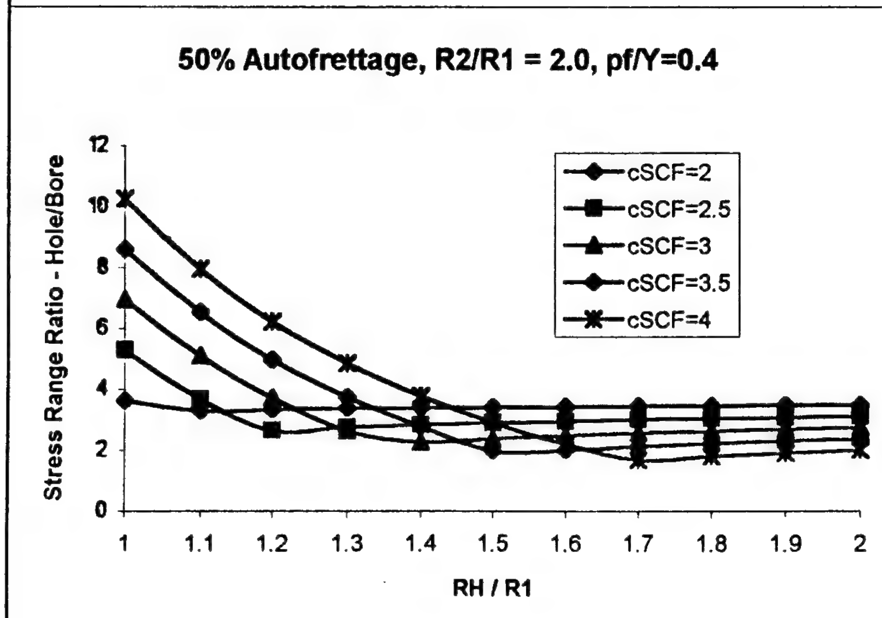
50% Autofrettage, R2/R1 = 2.0, pf/Y=0.4
cSCF=2
cSCF=2.5
cSCF=3
cSCF=3.5
cSCF=4
Stress Range Ratio - Hole/Bore
RH / R1

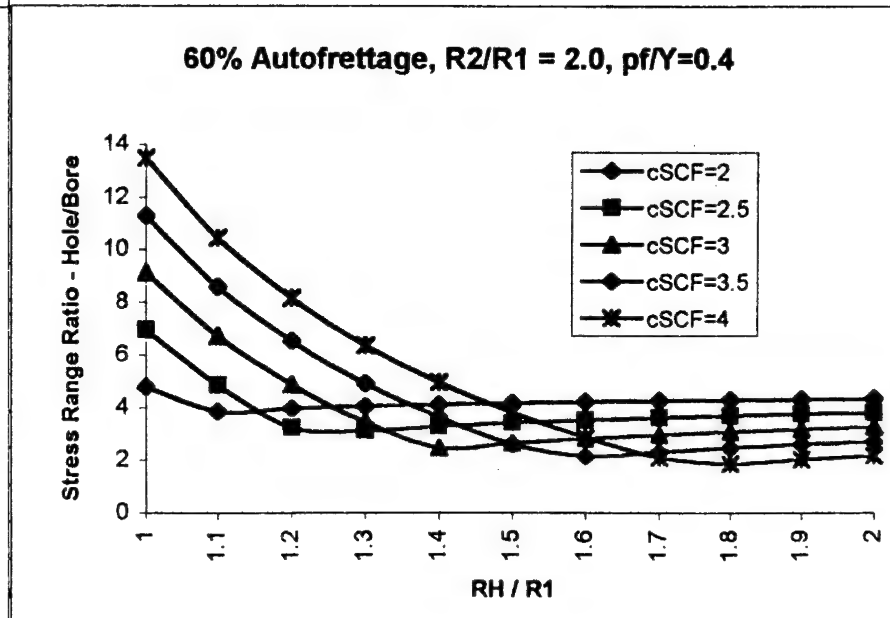
60% Autofrettage, R2/R1 = 2.0, pf/Y=0.4
cSCF=2
cSCF=2.5
cSCF=3
cSCF=3.5
cSCF=4
Stress Range Ratio - Hole/Bore
RH / R1

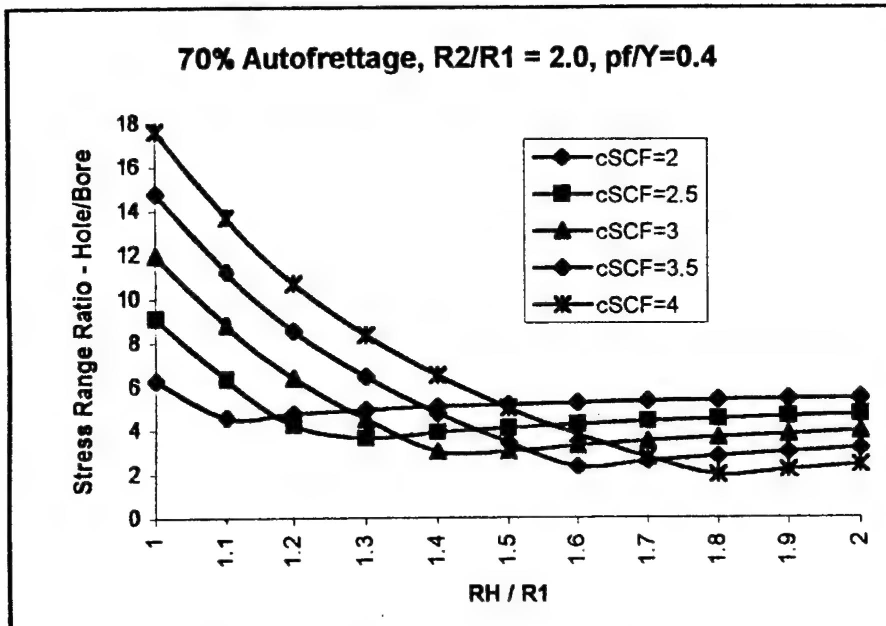
70% Autofrettage, R2/R1 = 2.0, pf/Y=0.4
Stress Range Ratio - Hole/Bore
RH / R1
cSCF=2
cSCF=2.5
cSCF=3
cSCF=3.5
cSCF=4

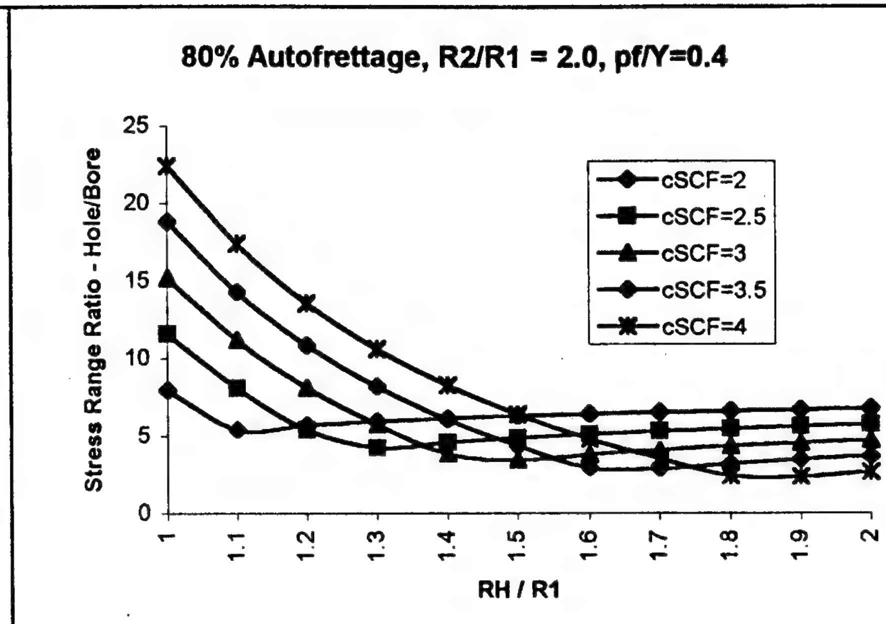
80% Autofrettage, R2/R1 = 2.0, pf/Y=0.4
Stress Range Ratio - Hole/Bore
RH / R1
cSCF=2
cSCF=2.5
cSCF=3
cSCF=3.5
cSCF=4

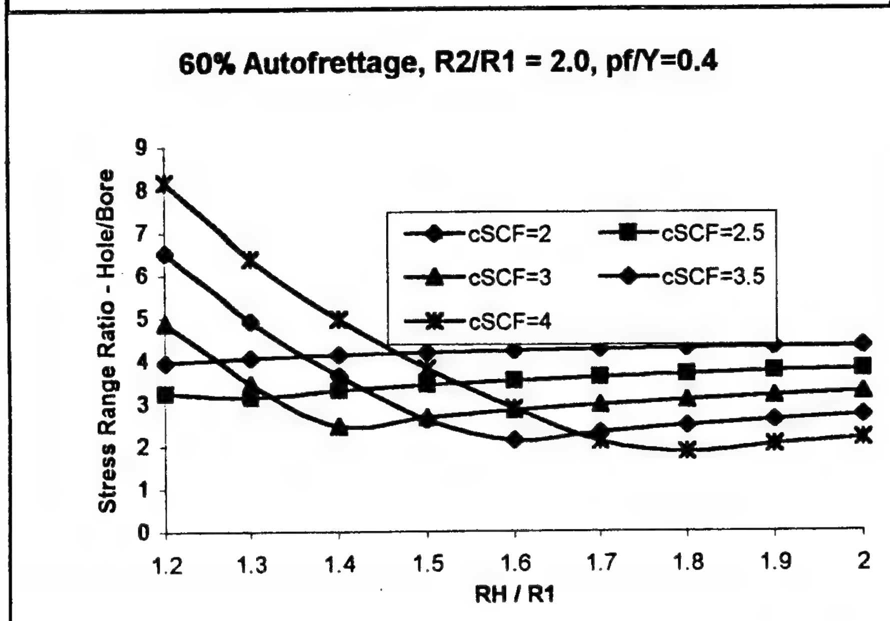
60% Autofrettage, R2/R1 = 2.0, pf/Y=0.4
Stress Range Ratio - Hole/Bore
RH / R1
cSCF=2
cSCF=2.5
cSCF=3
cSCF=3.5
cSCF=4

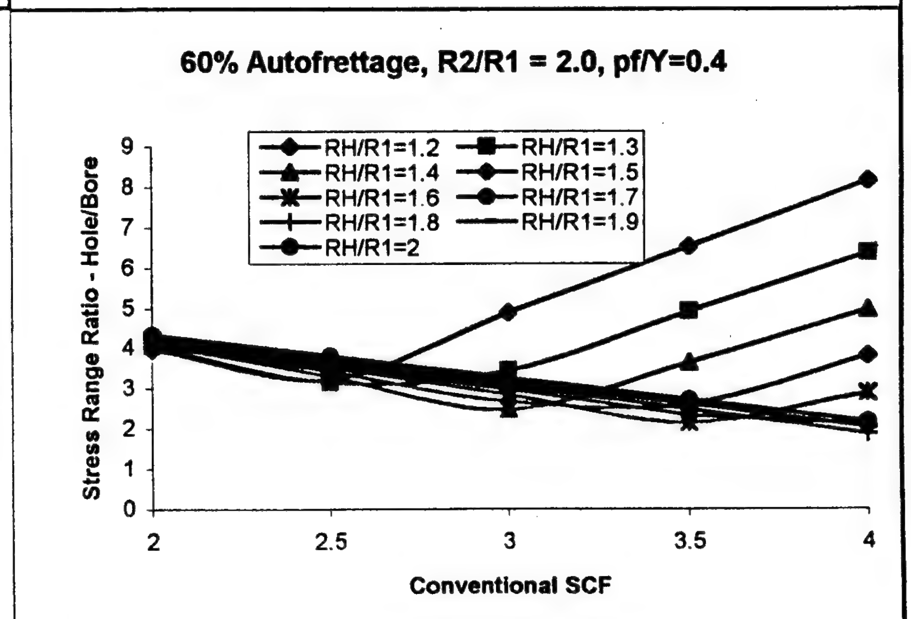
60% Autofrettage, R2/R1 = 2.0, pf/Y=0.4
Stress Range Ratio - Hole/Bore
Conventional SCF
RH/R1=1.2
RH/R1=1.3
RH/R1=1.4
RH/R1=1.5
RH/R1=1.6
RH/R1=1.7
RH/R1=1.8
RH/R1=1.9
RH/R1=2

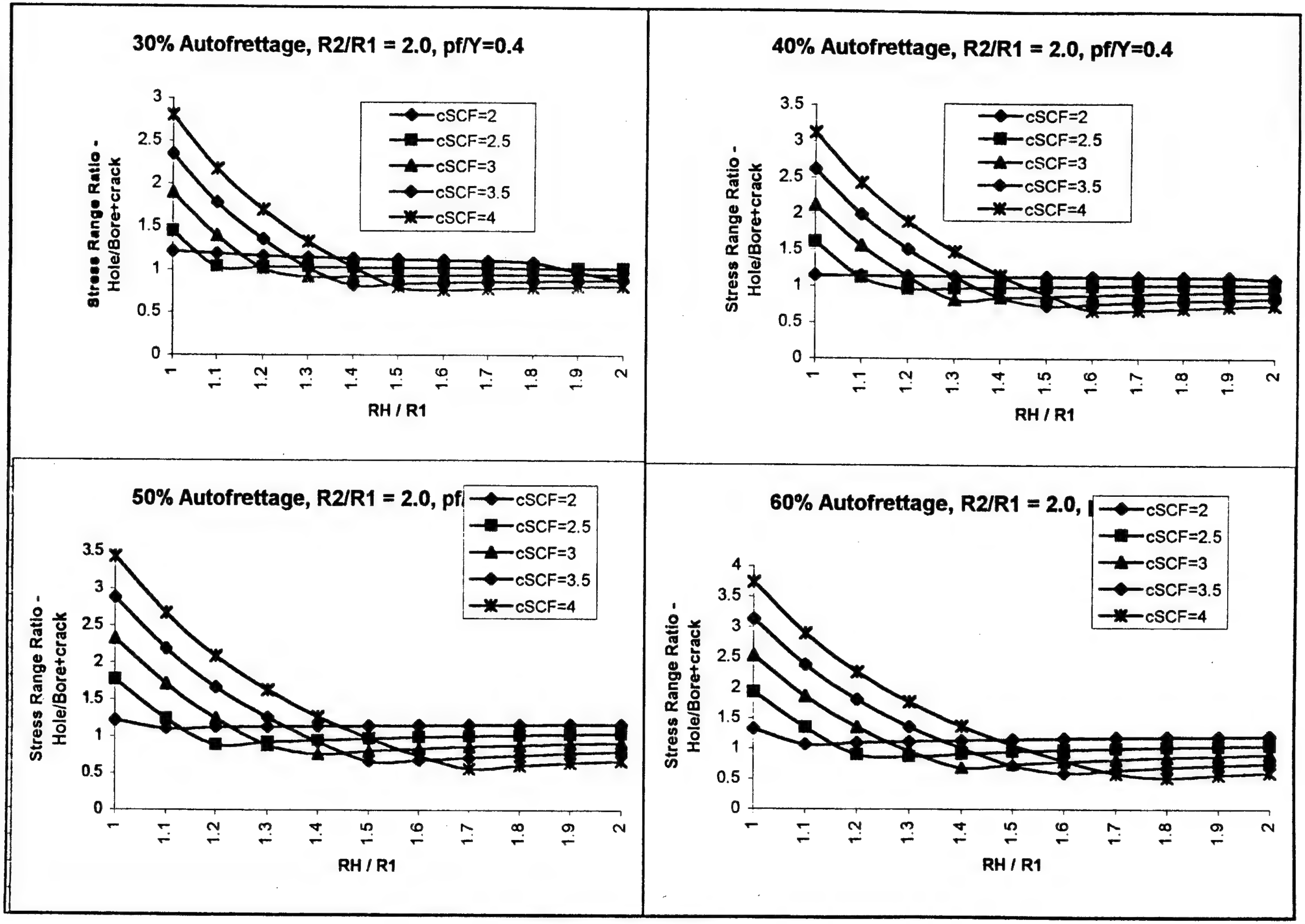
30% Autofrettage, R2/R1 = 2.0, pf/Y=0.4
Stress Range Ratio - Hole/Bore+crack
RH / R1
cSCF=2
cSCF=2.5
cSCF=3
cSCF=3.5
cSCF=4
40% Autofrettage, R2/R1 = 2.0, pf/Y=0.4
Stress Range Ratio - Hole/Bore+crack
RH / R1
cSCF=2
cSCF=2.5
cSCF=3
cSCF=3.5
cSCF=4
50% Autofrettage, R2/R1 = 2.0, pf
Stress Range Ratio - Hole/Bore+crack
RH / R1
cSCF=2
cSCF=2.5
cSCF=3
cSCF=3.5
cSCF=4
60% Autofrettage, R2/R1 = 2.0,
Stress Range Ratio - Hole/Bore+crack
RH / R1
cSCF=2
cSCF=2.5
cSCF=3
cSCF=3.5
cSCF=4

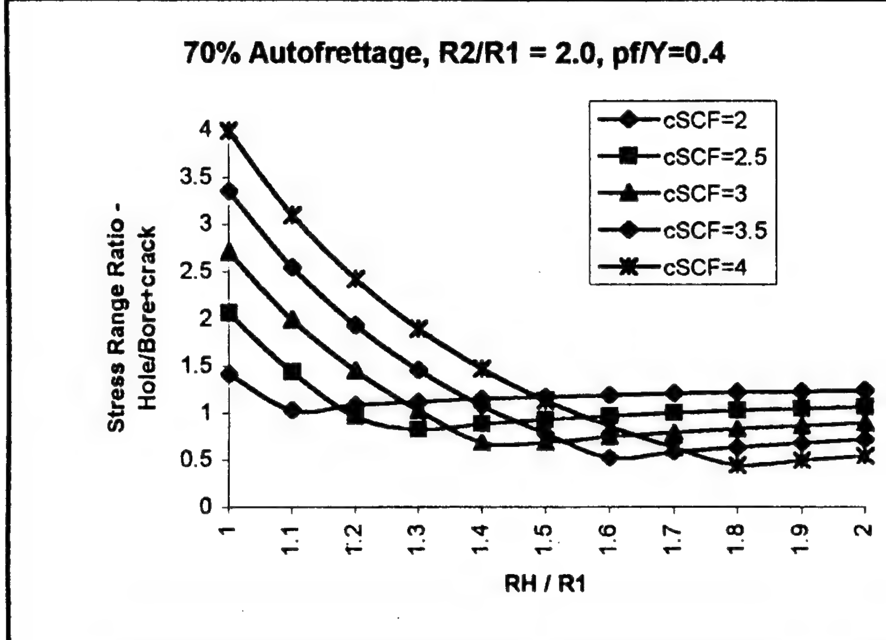
70% Autofrettage, R2/R1 = 2.0, pf/Y=0.4
cSCF=2
cSCF=2.5
cSCF=3
cSCF=3.5
cSCF=4
Stress Range Ratio - Hole/Bore+crack
RH / R1

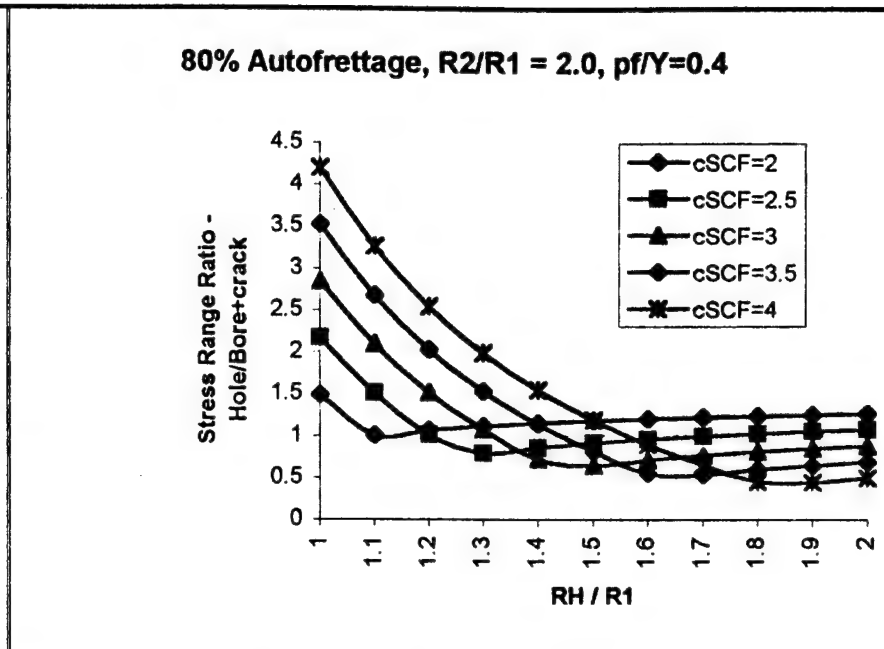
80% Autofrettage, R2/R1 = 2.0, pf/Y=0.4
cSCF=2
cSCF=2.5
cSCF=3
cSCF=3.5
cSCF=4
Stress Range Ratio - Hole/Bore+crack
RH / R1

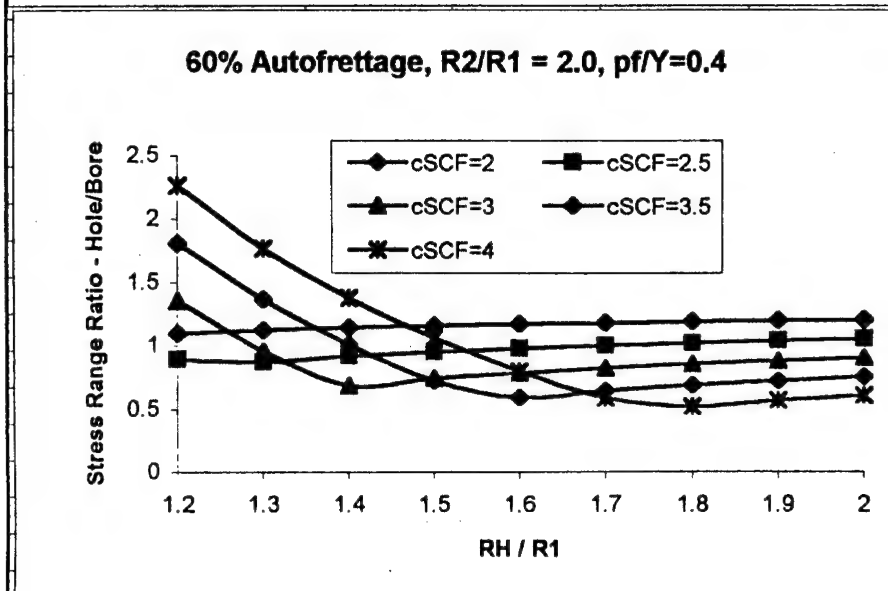
60% Autofrettage, R2/R1 = 2.0, pf/Y=0.4
cSCF=2
cSCF=2.5
cSCF=3
cSCF=3.5
cSCF=4
Stress Range Ratio - Hole/Bore
RH / R1

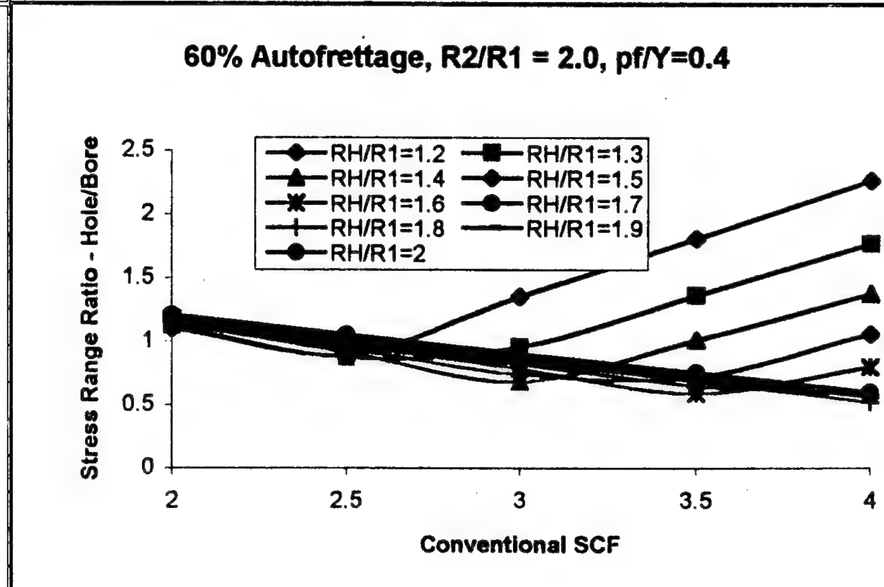
60% Autofrettage, R2/R1 = 2.0, pf/Y=0.4
RH/R1=1.2
RH/R1=1.3
RH/R1=1.4
RH/R1=1.5
RH/R1=1.6
RH/R1=1.7
RH/R1=1.8
RH/R1=1.9
RH/R1=2
Stress Range Ratio - Hole/Bore
Conventional SCF

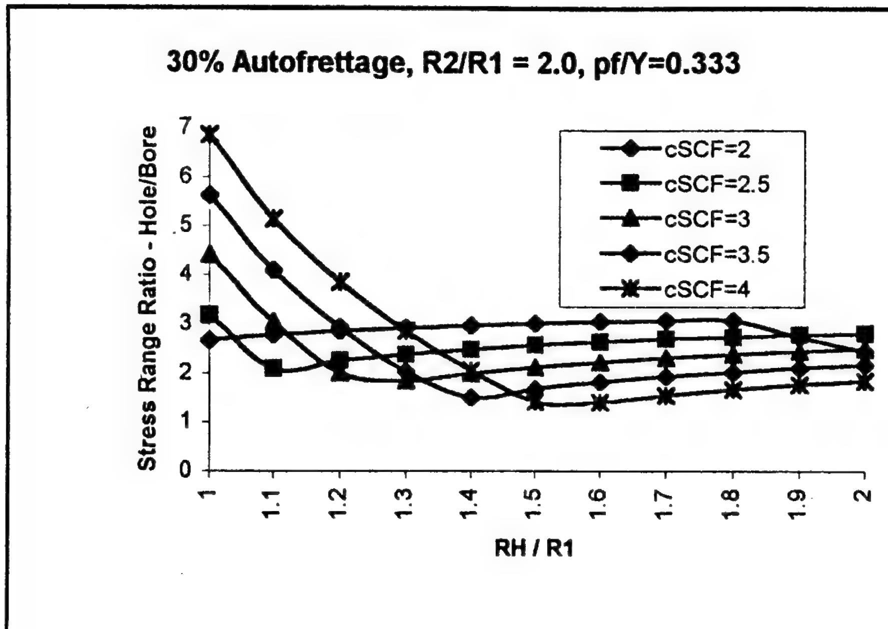
30% Autofrettage, R2/R1 = 2.0, pf/Y=0.333
Stress Range Ratio - Hole/Bore
RH / R1
cSCF=2
cSCF=2.5
cSCF=3
cSCF=3.5
cSCF=4

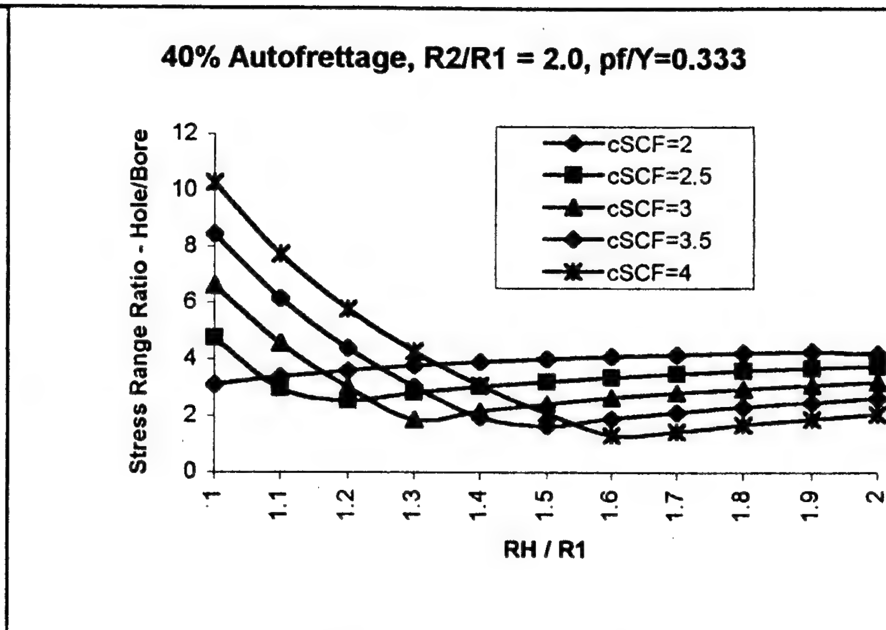
40% Autofrettage, R2/R1 = 2.0, pf/Y=0.333
Stress Range Ratio - Hole/Bore
RH / R1
cSCF=2
cSCF=2.5
cSCF=3
cSCF=3.5
cSCF=4

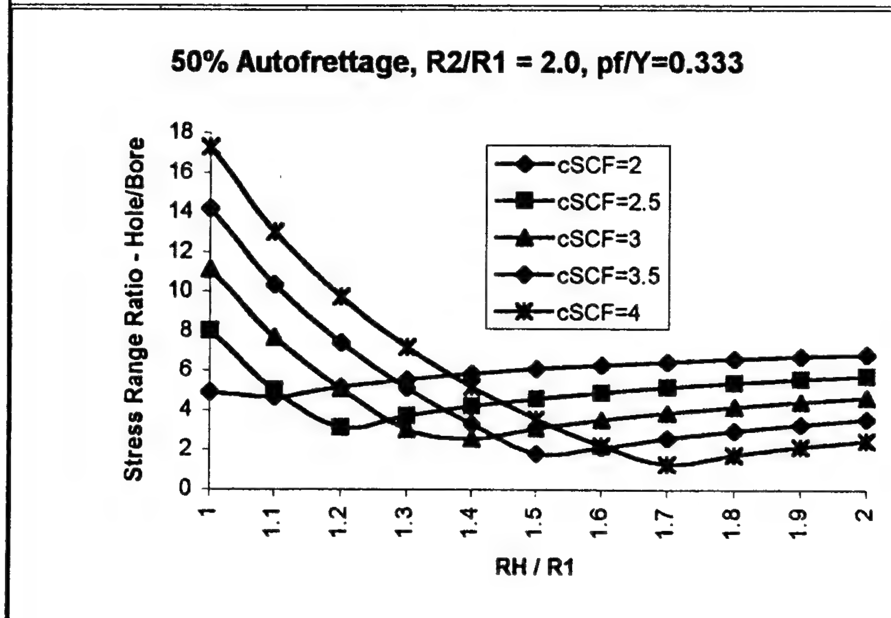
50% Autofrettage, R2/R1 = 2.0, pf/Y=0.333
Stress Range Ratio - Hole/Bore
RH / R1
cSCF=2
cSCF=2.5
cSCF=3
cSCF=3.5
cSCF=4

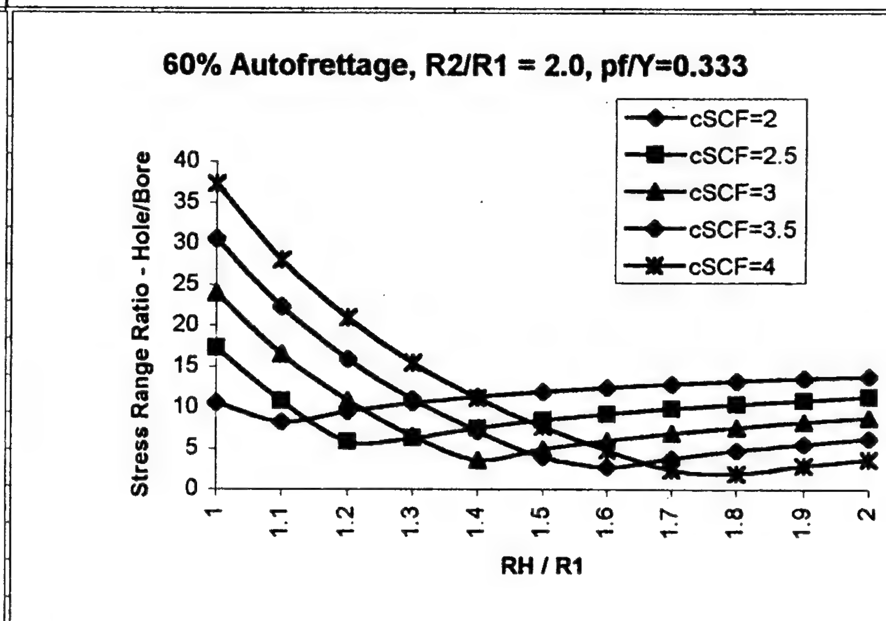
60% Autofrettage, R2/R1 = 2.0, pf/Y=0.333
Stress Range Ratio - Hole/Bore
RH / R1
cSCF=2
cSCF=2.5
cSCF=3
cSCF=3.5
cSCF=4

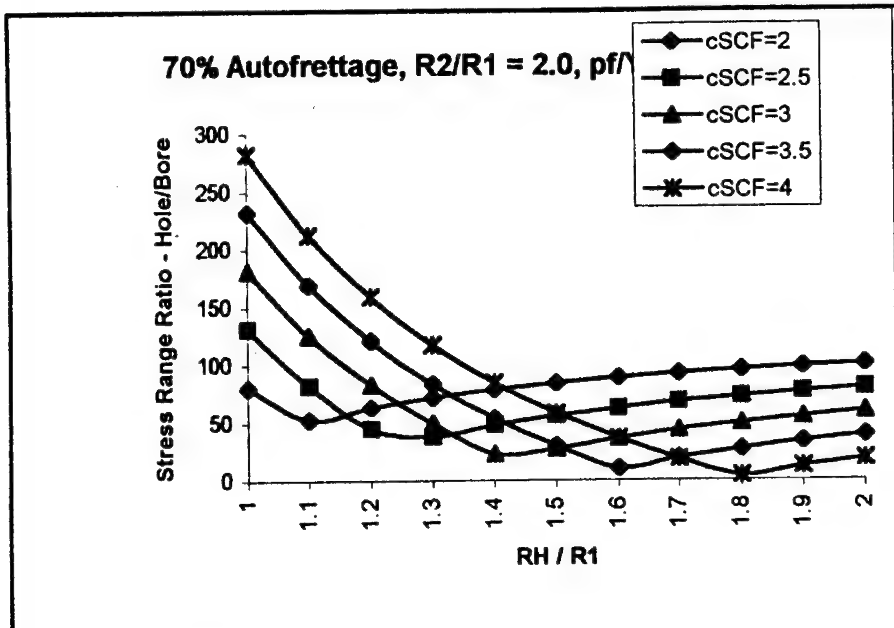
70% Autofrettage, R2/R1 = 2.0, pf/Y
cSCF=2
cSCF=2.5
cSCF=3
cSCF=3.5
cSCF=4
Stress Range Ratio - Hole/Bore
RH / R1

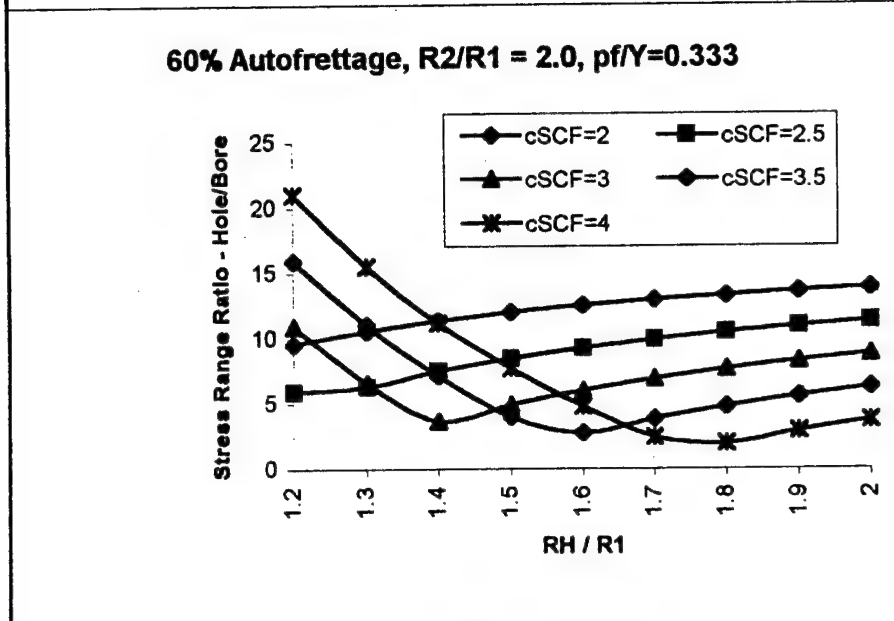
60% Autofrettage, R2/R1 = 2.0, pf/Y=0.333
cSCF=2
cSCF=2.5
cSCF=3
cSCF=3.5
cSCF=4
Stress Range Ratio - Hole/Bore
RH / R1

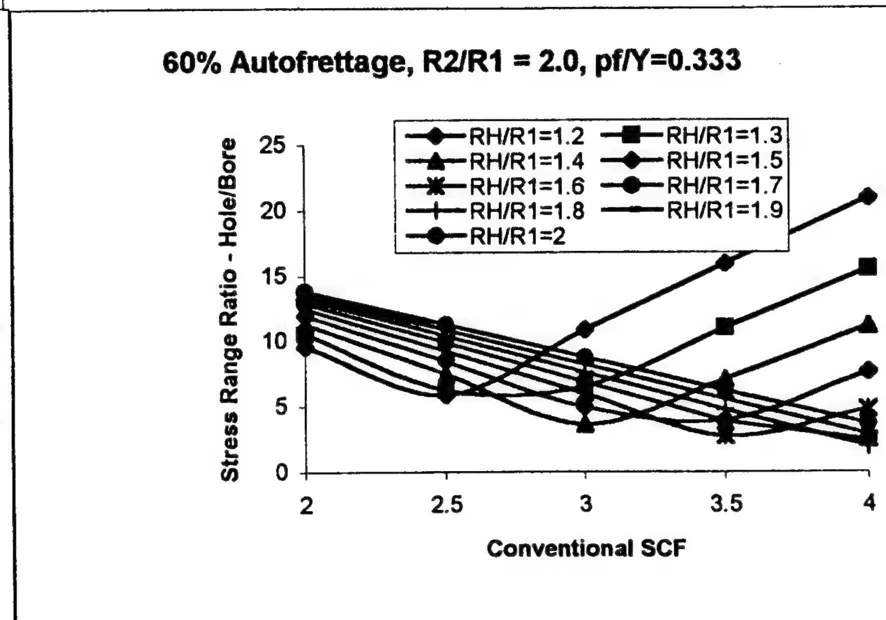
60% Autofrettage, R2/R1 = 2.0, pf/Y=0.333
RH/R1=1.2
RH/R1=1.3
RH/R1=1.4
RH/R1=1.5
RH/R1=1.6
RH/R1=1.7
RH/R1=1.8
RH/R1=1.9
RH/R1=2
Stress Range Ratio - Hole/Bore
Conventional SCF

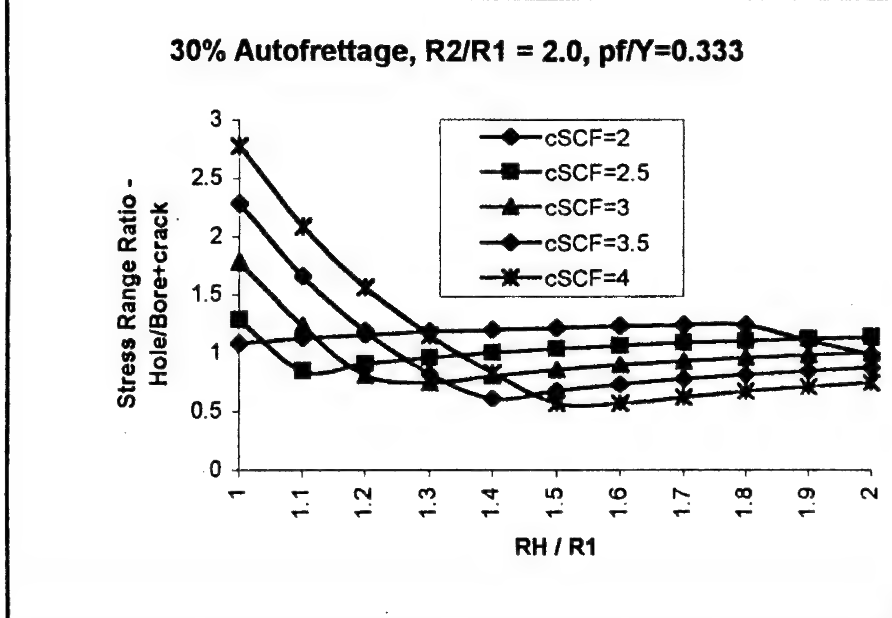
30% Autofrettage, R2/R1 = 2.0, pf/Y=0.333
Stress Range Ratio - Hole/Bore+crack
RH / R1
cSCF=2
cSCF=2.5
cSCF=3
cSCF=3.5
cSCF=4

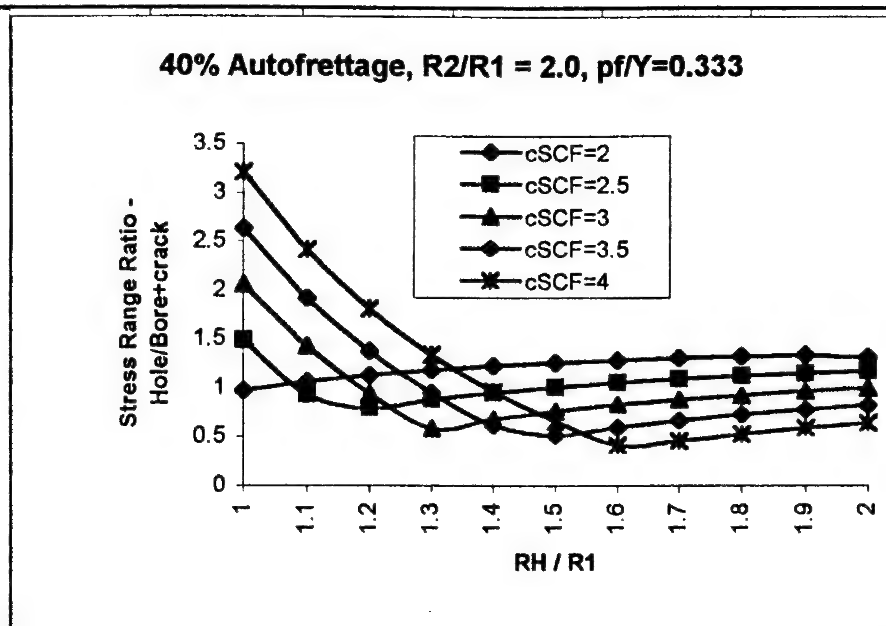
40% Autofrettage, R2/R1 = 2.0, pf/Y=0.333
Stress Range Ratio - Hole/Bore+crack
RH / R1
cSCF=2
cSCF=2.5
cSCF=3
cSCF=3.5
cSCF=4

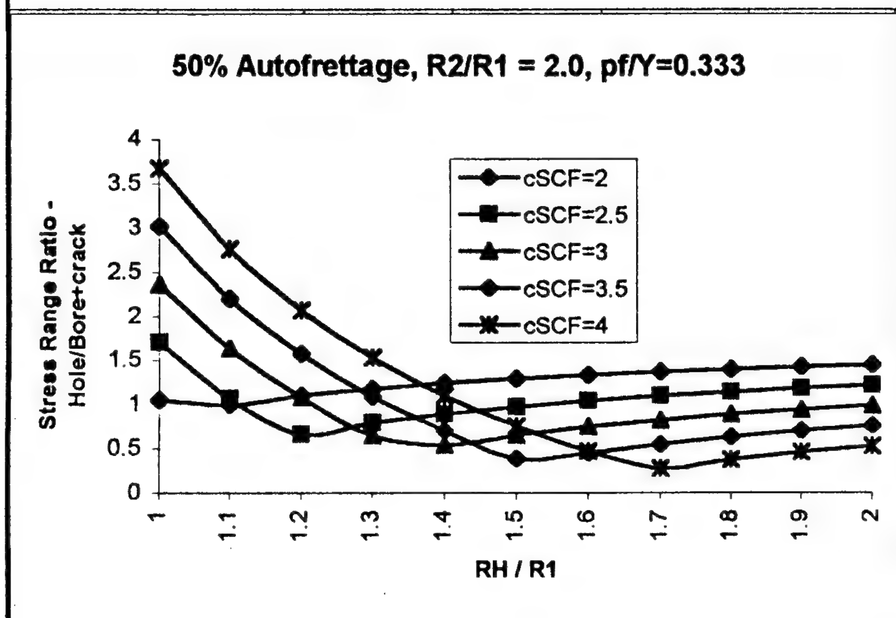
50% Autofrettage, R2/R1 = 2.0, pf/Y=0.333
Stress Range Ratio - Hole/Bore+crack
RH / R1
cSCF=2
cSCF=2.5
cSCF=3
cSCF=3.5
cSCF=4

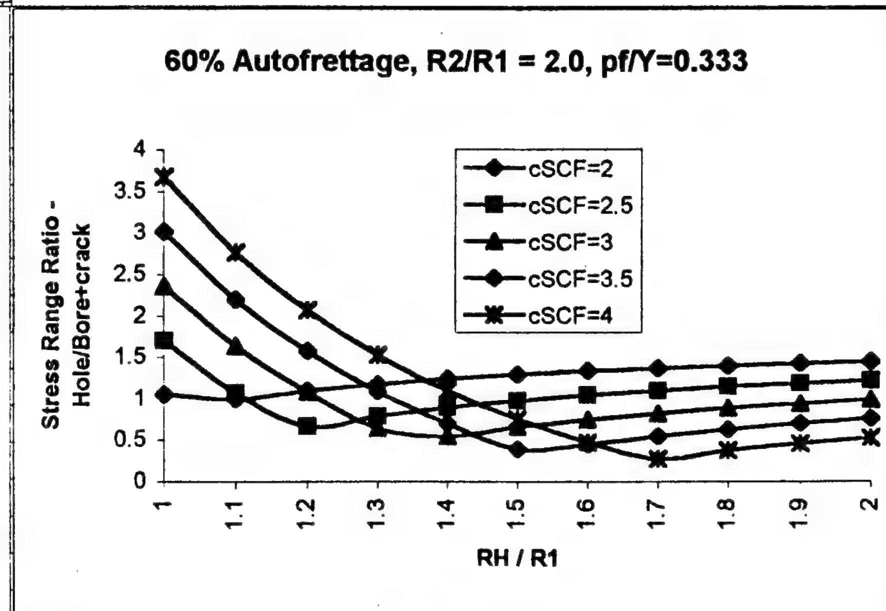
60% Autofrettage, R2/R1 = 2.0, pf/Y=0.333
Stress Range Ratio - Hole/Bore+crack
RH / R1
cSCF=2
cSCF=2.5
cSCF=3
cSCF=3.5
cSCF=4

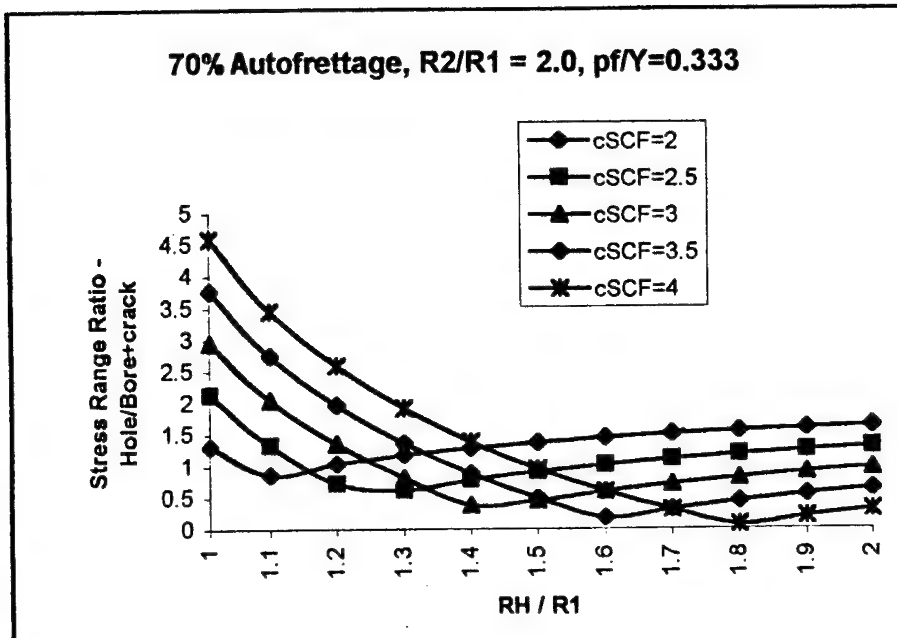
70% Autofrettage, R2/R1 = 2.0, pf/Y=0.333
cSCF=2
cSCF=2.5
cSCF=3
cSCF=3.5
cSCF=4
Stress Range Ratio - Hole/Bore+crack
RH / R1

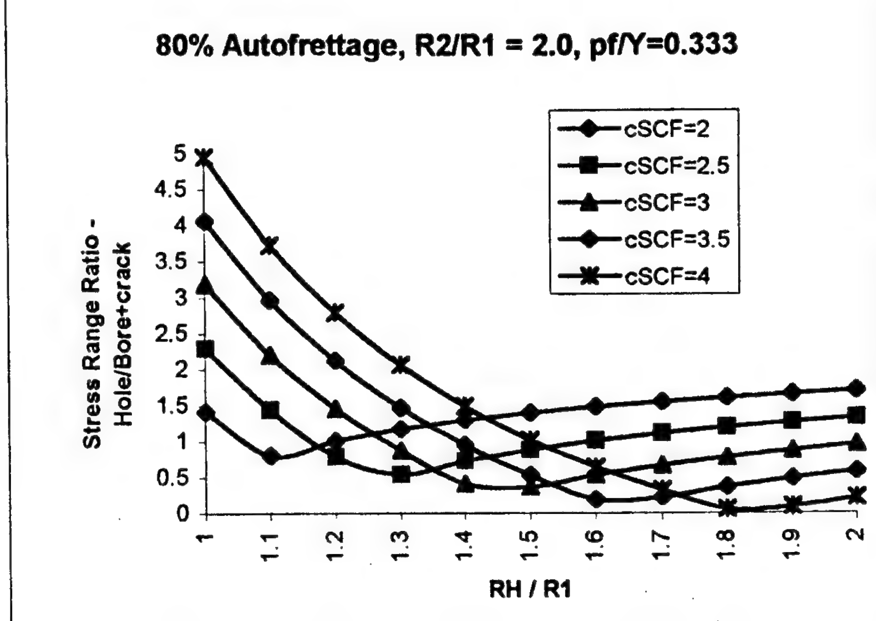
80% Autofrettage, R2/R1 = 2.0, pf/Y=0.333
cSCF=2
cSCF=2.5
cSCF=3
cSCF=3.5
cSCF=4
Stress Range Ratio - Hole/Bore+crack
RH / R1

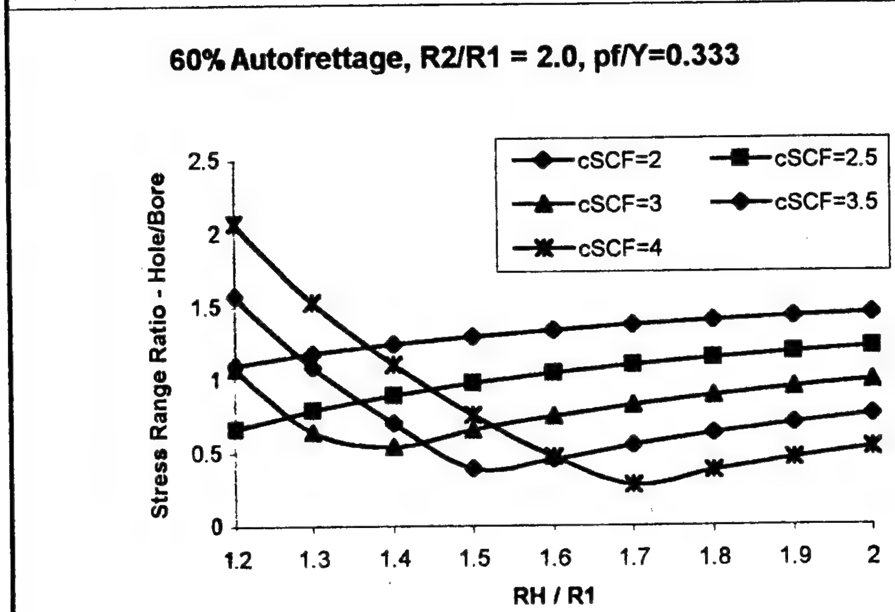
60% Autofrettage, R2/R1 = 2.0, pf/Y=0.333
cSCF=2
cSCF=2.5
cSCF=3
cSCF=3.5
cSCF=4
Stress Range Ratio - Hole/Bore
RH / R1

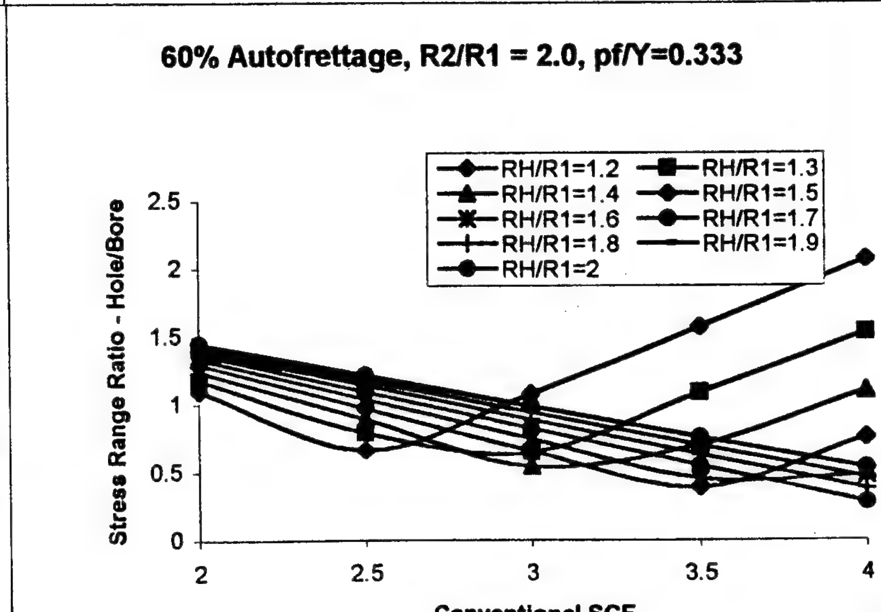
60% Autofrettage, R2/R1 = 2.0, pf/Y=0.333
RH/R1=1.2
RH/R1=1.3
RH/R1=1.4
RH/R1=1.5
RH/R1=1.6
RH/R1=1.7
RH/R1=1.8
RH/R1=1.9
RH/R1=2
Stress Range Ratio - Hole/Bore
Conventional SCF

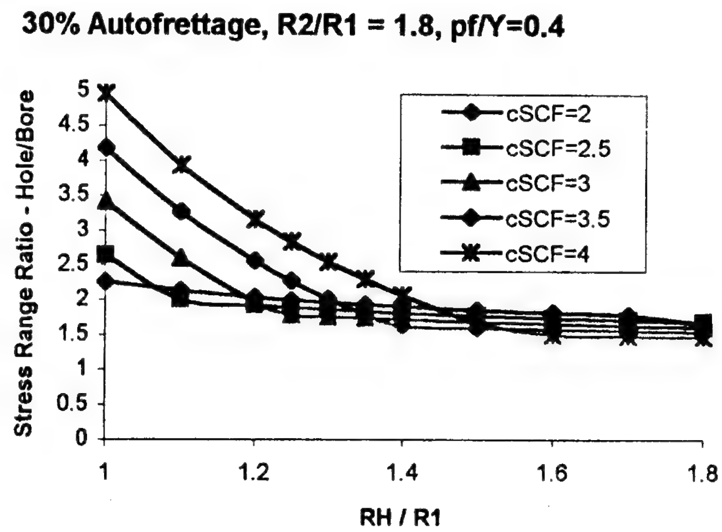
30% Autofrettage, R2/R1 = 1.8, pf/Y=0.4
Stress Range Ratio - Hole/Bore
RH / R1
cSCF=2
cSCF=2.5
cSCF=3
cSCF=3.5
cSCF=4

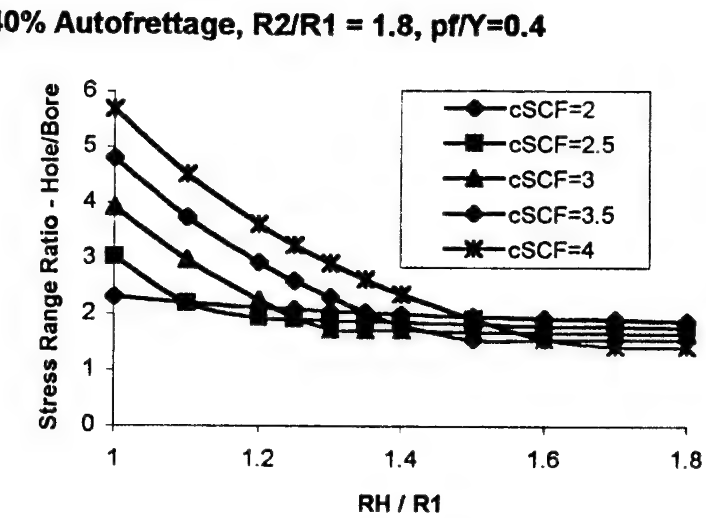
40% Autofrettage, R2/R1 = 1.8, pf/Y=0.4
Stress Range Ratio - Hole/Bore
RH / R1
cSCF=2
cSCF=2.5
cSCF=3
cSCF=3.5
cSCF=4

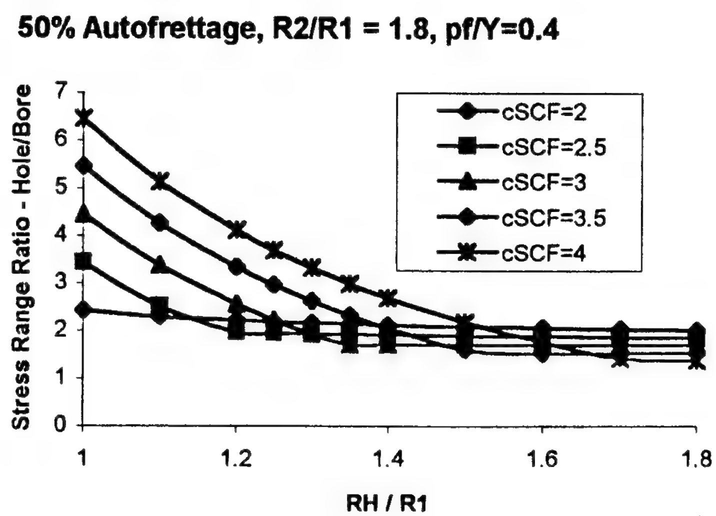
50% Autofrettage, R2/R1 = 1.8, pf/Y=0.4
Stress Range Ratio - Hole/Bore
RH / R1
cSCF=2
cSCF=2.5
cSCF=3
cSCF=3.5
cSCF=4

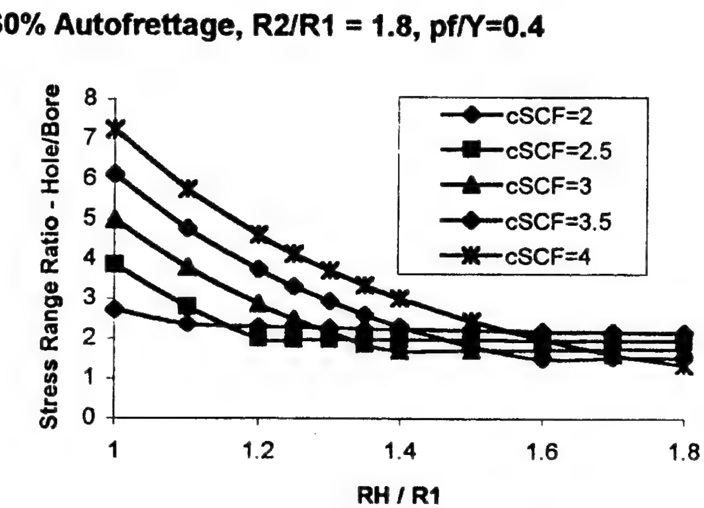
60% Autofrettage, R2/R1 = 1.8, pf/Y=0.4
Stress Range Ratio - Hole/Bore
RH / R1
cSCF=2
cSCF=2.5
cSCF=3
cSCF=3.5
cSCF=4

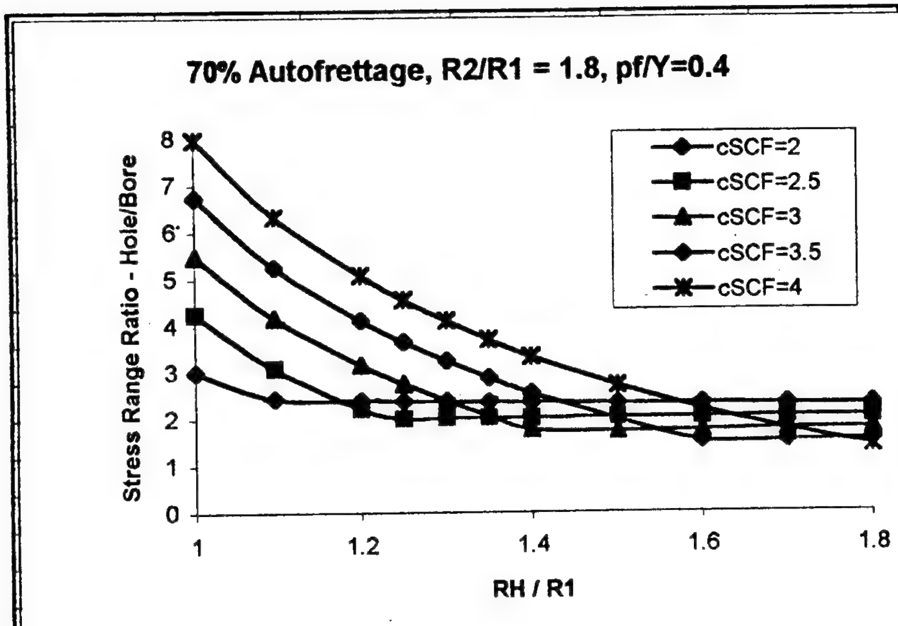
70% Autofrettage, R2/R1 = 1.8, pf/Y=0.4
Stress Range Ratio - Hole/Bore
RH / R1
cSCF=2
cSCF=2.5
cSCF=3
cSCF=3.5
cSCF=4

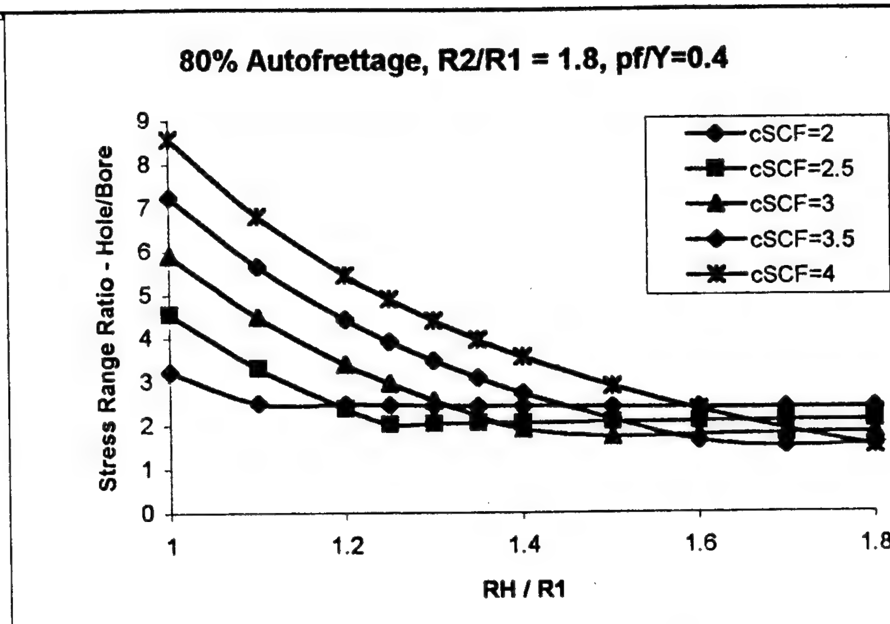
80% Autofrettage, R2/R1 = 1.8, pf/Y=0.4
Stress Range Ratio - Hole/Bore
RH / R1
cSCF=2
cSCF=2.5
cSCF=3
cSCF=3.5
cSCF=4

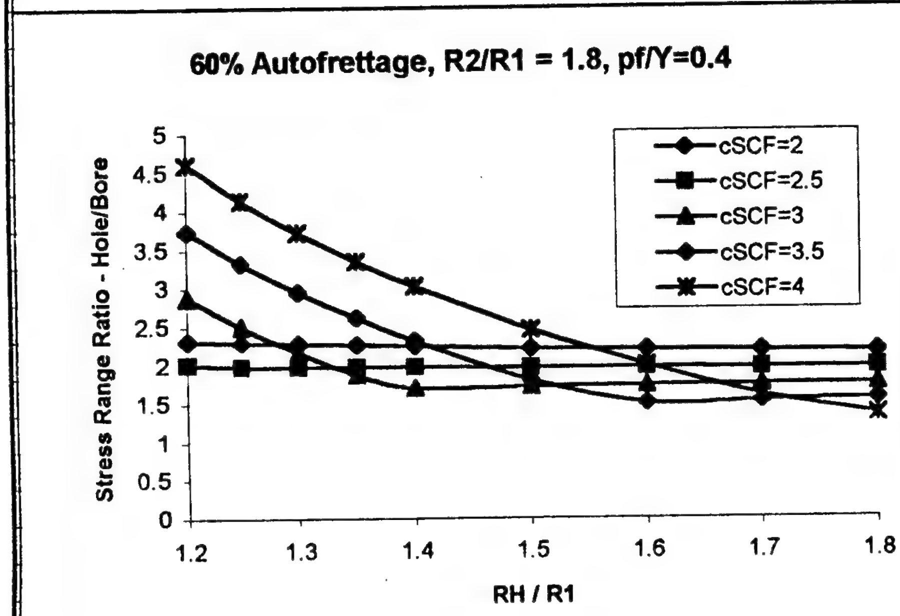
60% Autofrettage, R2/R1 = 1.8, pf/Y=0.4
Stress Range Ratio - Hole/Bore
RH / R1
cSCF=2
cSCF=2.5
cSCF=3
cSCF=3.5
cSCF=4

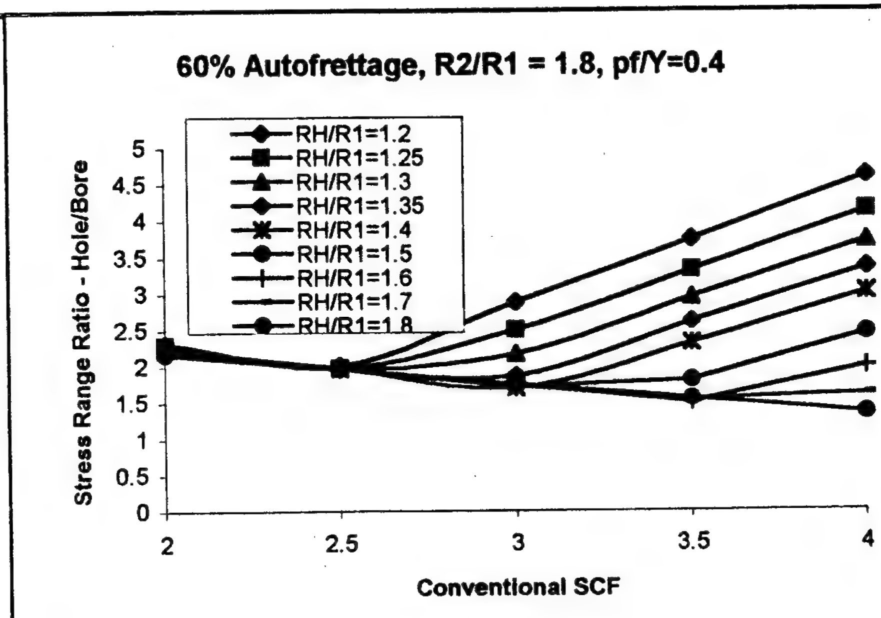
60% Autofrettage, R2/R1 = 1.8, pf/Y=0.4
Stress Range Ratio - Hole/Bore
Conventional SCF
RH/R1=1.2
RH/R1=1.25
RH/R1=1.3
RH/R1=1.35
RH/R1=1.4
RH/R1=1.5
RH/R1=1.6
RH/R1=1.7
RH/R1=1.8

30% Autofrettage, R2/R1 = 1.8, pf/Y=0.4

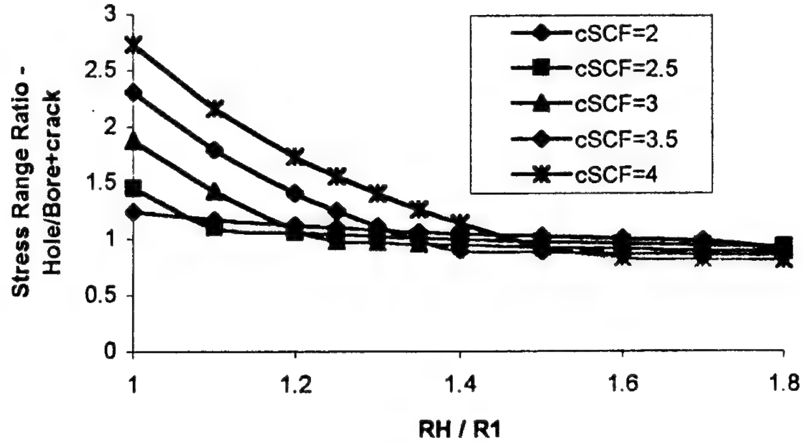

40% Autofrettage, R2/R1 = 1.8, pf/Y=0.4

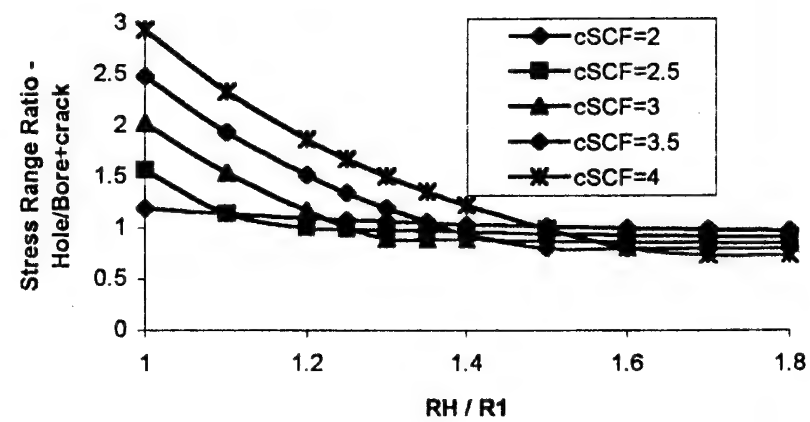

50% Autofrettage, R2/R1 = 1.8, pf/Y=0.4

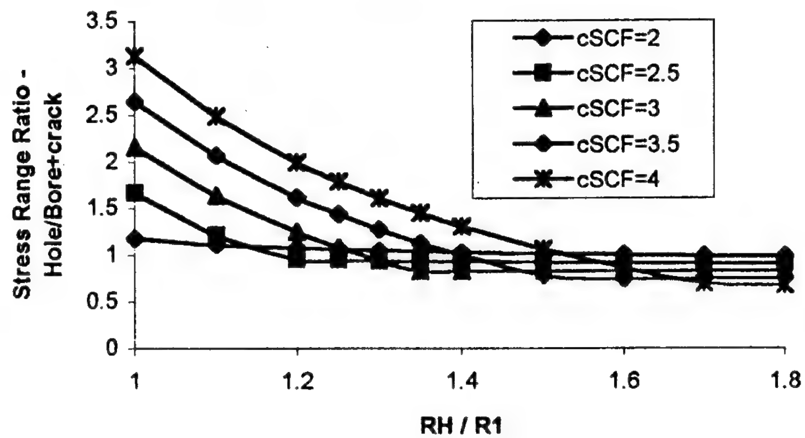

60% Autofrettage, R2/R1 = 1.8, pf/Y=0.4

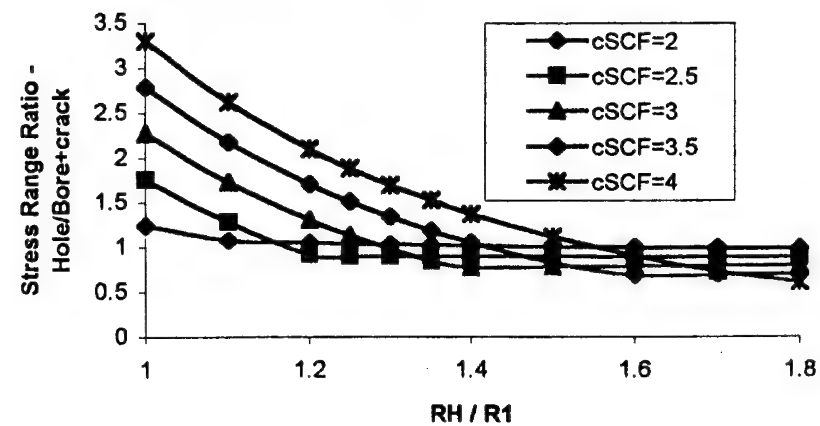

70% Autofrettage, R2/R1 = 1.8, pf/Y=0.4

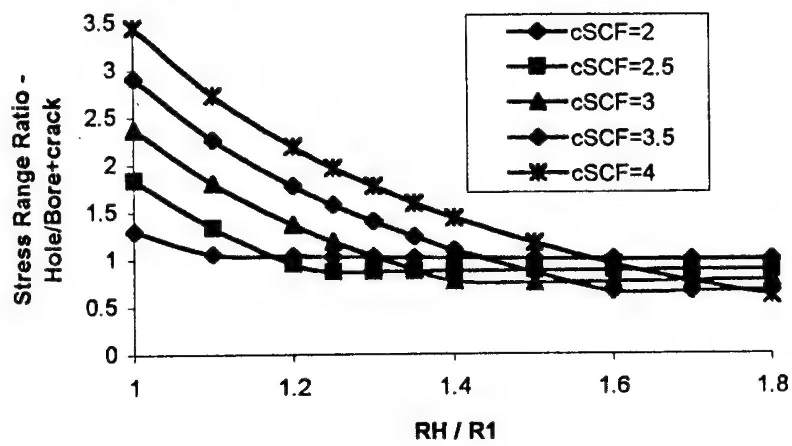

80% Autofrettage, R2/R1 = 1.8, pf/Y=0.4

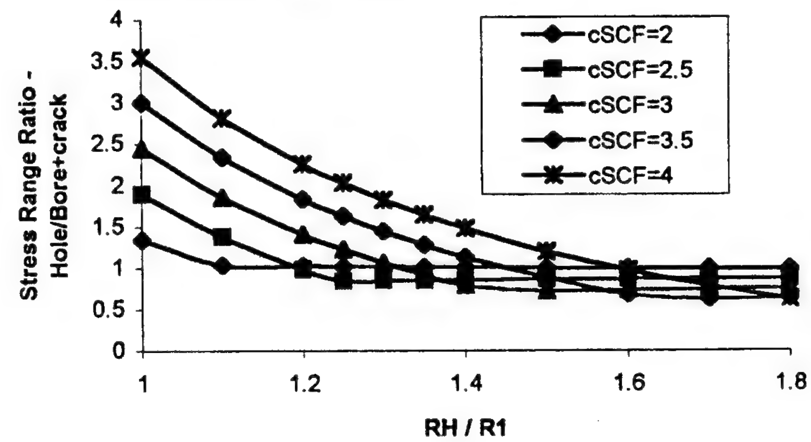

60% Autofrettage, R2/R1 = 1.8, pf/Y=0.4

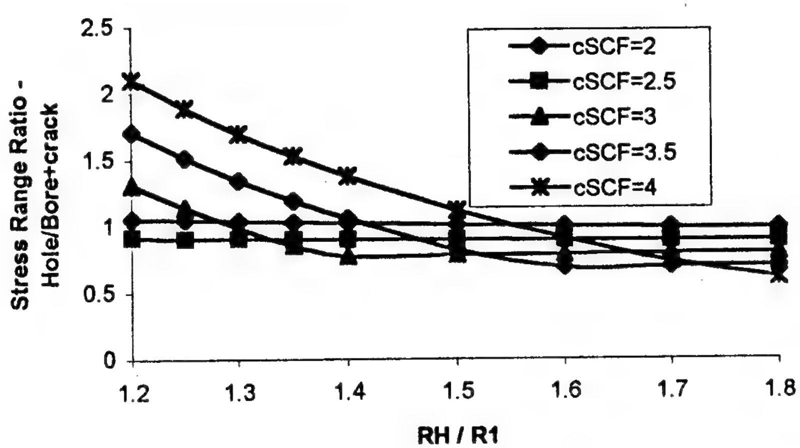

60% Autofrettage, R2/R1 = 1.8, pf/Y=0.4

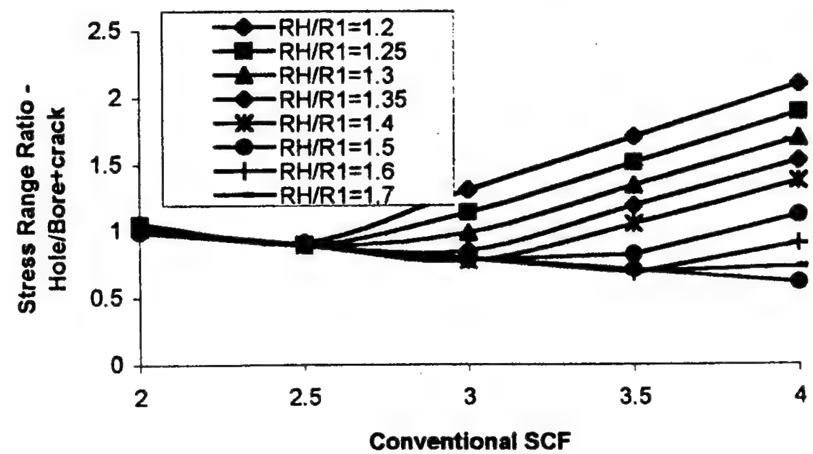

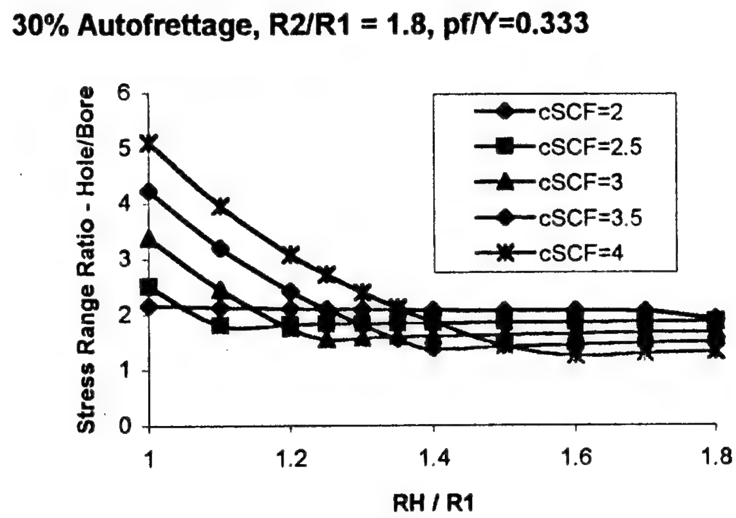
30% Autofrettage, R2/R1 = 1.8, pf/Y=0.333
Stress Range Ratio - Hole/Bore
RH / R1
cSCF=2
cSCF=2.5
cSCF=3
cSCF=3.5
cSCF=4
0
1
2
3
4
5
6
1
1.2
1.4
1.6
1.8

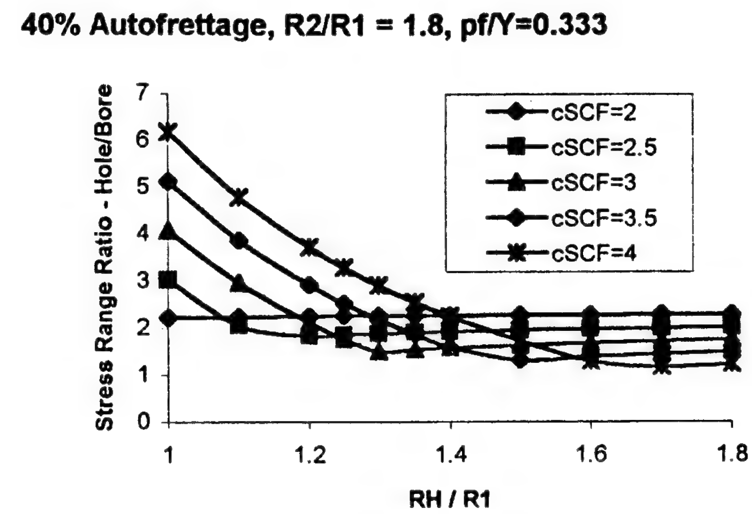
40% Autofrettage, R2/R1 = 1.8, pf/Y=0.333
Stress Range Ratio - Hole/Bore
RH / R1
cSCF=2
cSCF=2.5
cSCF=3
cSCF=3.5
cSCF=4
0
1
2
3
4
5
6
7
1
1.2
1.4
1.6
1.8

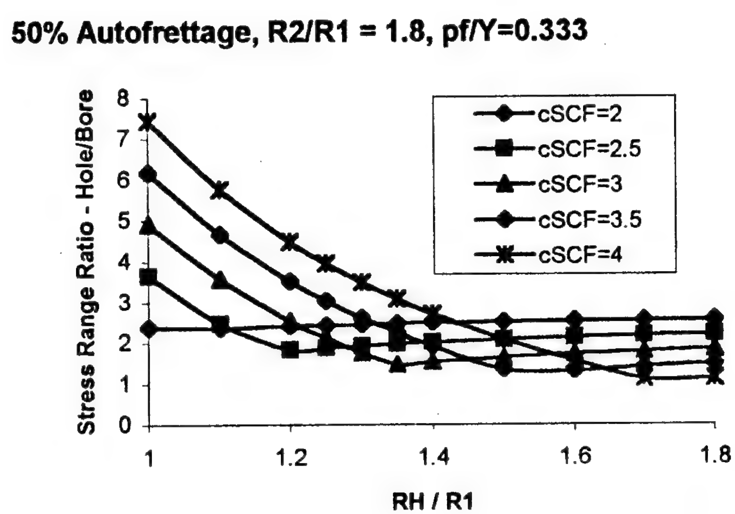
50% Autofrettage, R2/R1 = 1.8, pf/Y=0.333
Stress Range Ratio - Hole/Bore
RH / R1
cSCF=2
cSCF=2.5
cSCF=3
cSCF=3.5
cSCF=4
0
1
2
3
4
5
6
7
8
1
1.2
1.4
1.6
1.8

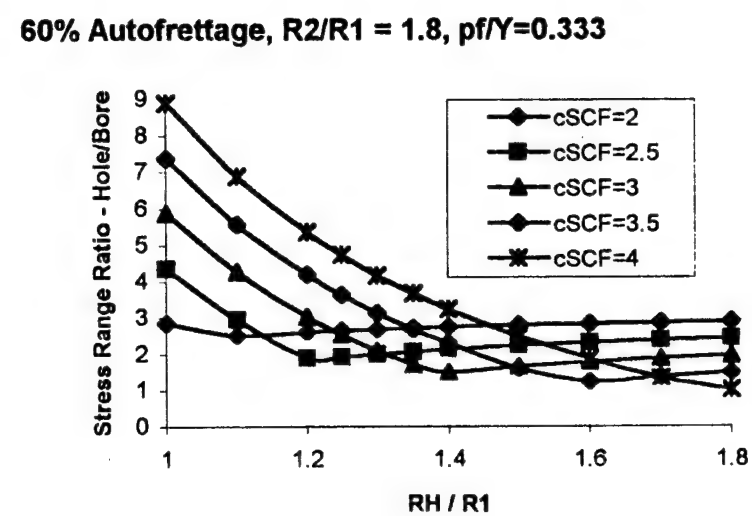
60% Autofrettage, R2/R1 = 1.8, pf/Y=0.333
Stress Range Ratio - Hole/Bore
RH / R1
cSCF=2
cSCF=2.5
cSCF=3
cSCF=3.5
cSCF=4
0
1
2
3
4
5
6
7
8
9
1
1.2
1.4
1.6
1.8

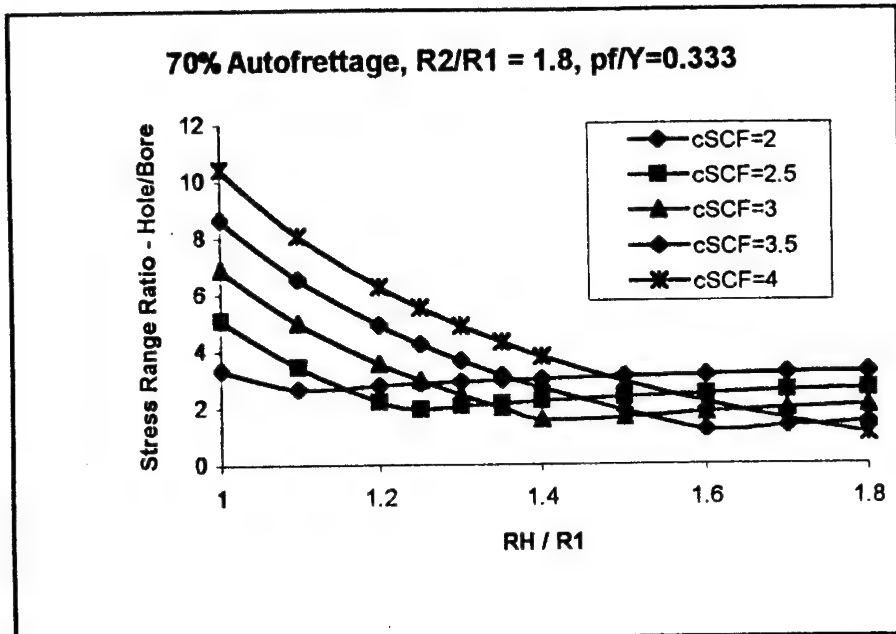
70% Autofrettage, R2/R1 = 1.8, pf/Y=0.333
Stress Range Ratio - Hole/Bore
RH / R1
cSCF=2
cSCF=2.5
cSCF=3
cSCF=3.5
cSCF=4

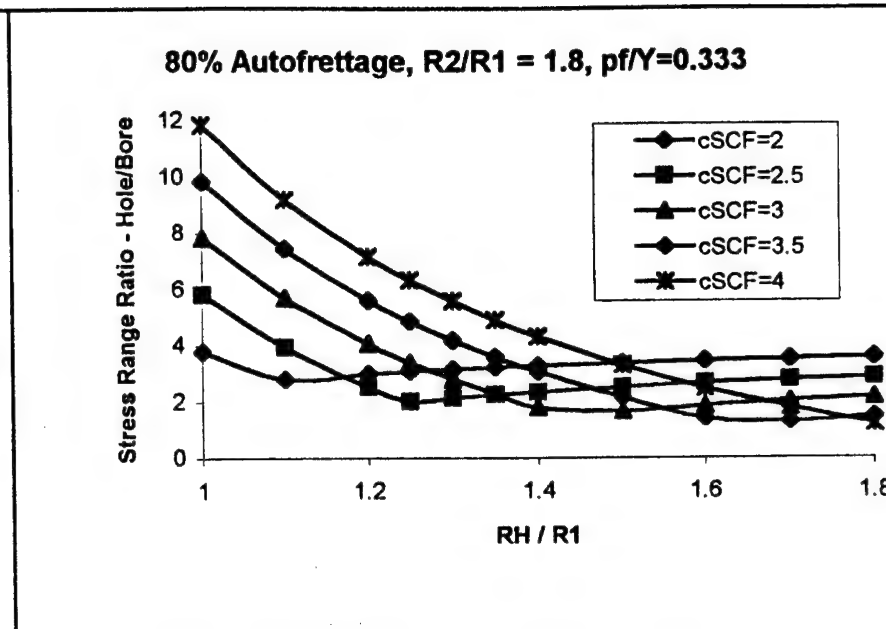
80% Autofrettage, R2/R1 = 1.8, pf/Y=0.333
Stress Range Ratio - Hole/Bore
RH / R1
cSCF=2
cSCF=2.5
cSCF=3
cSCF=3.5
cSCF=4

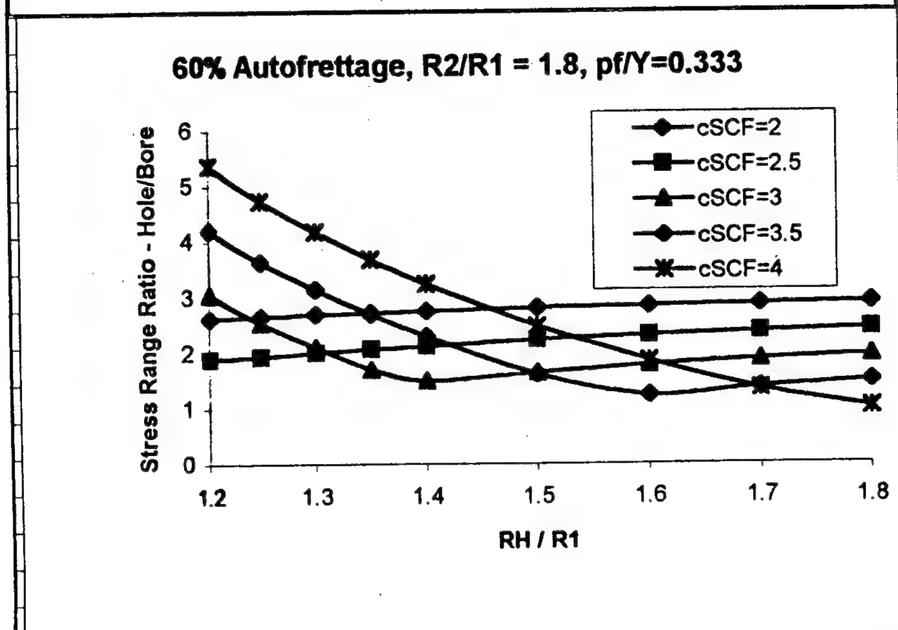
60% Autofrettage, R2/R1 = 1.8, pf/Y=0.333
Stress Range Ratio - Hole/Bore
RH / R1
cSCF=2
cSCF=2.5
cSCF=3
cSCF=3.5
cSCF=4

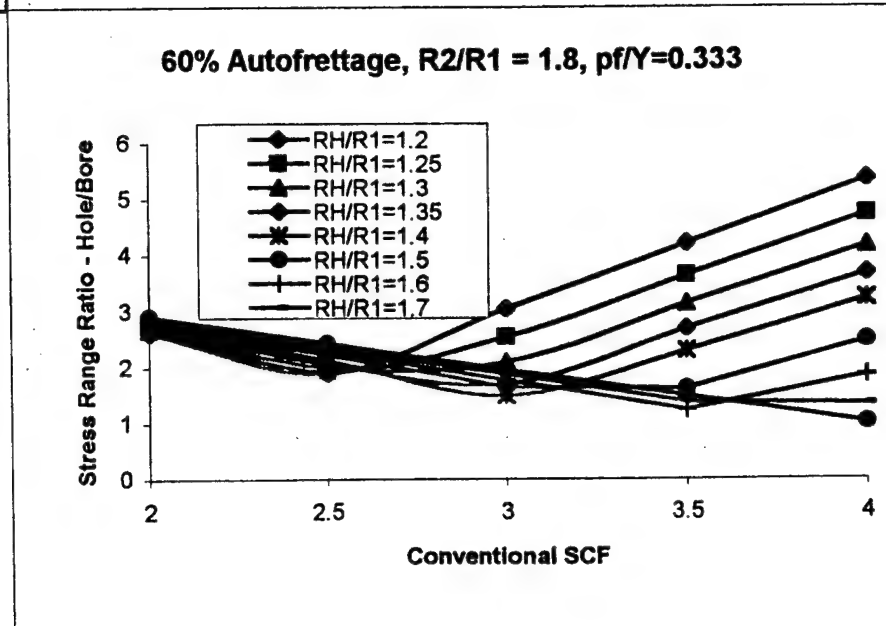
60% Autofrettage, R2/R1 = 1.8, pf/Y=0.333
Stress Range Ratio - Hole/Bore
Conventional SCF
RH/R1=1.2
RH/R1=1.25
RH/R1=1.3
RH/R1=1.35
RH/R1=1.4
RH/R1=1.5
RH/R1=1.6
RH/R1=1.7

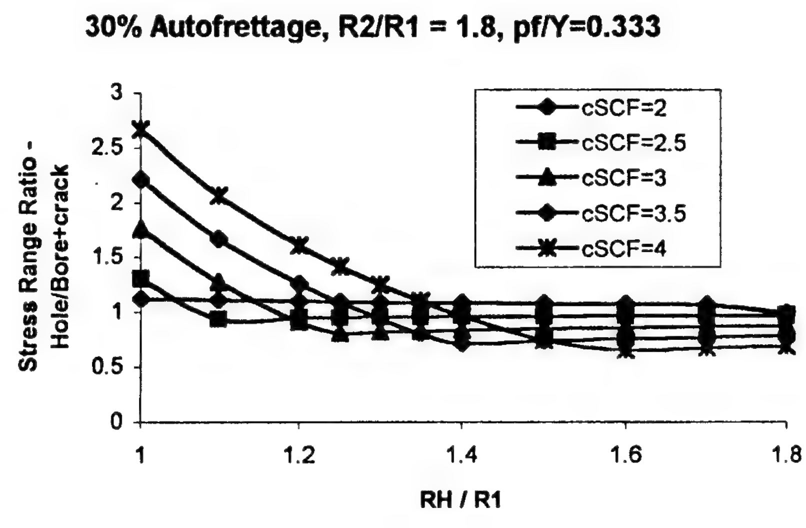
30% Autofrettage, R2/R1 = 1.8, pf/Y=0.333
Stress Range Ratio - Hole/Bore+crack
RH / R1
cSCF=2
cSCF=2.5
cSCF=3
cSCF=3.5
cSCF=4
0
0.5
1
1.5
2
2.5
3
1
1.2
1.4
1.6
1.8

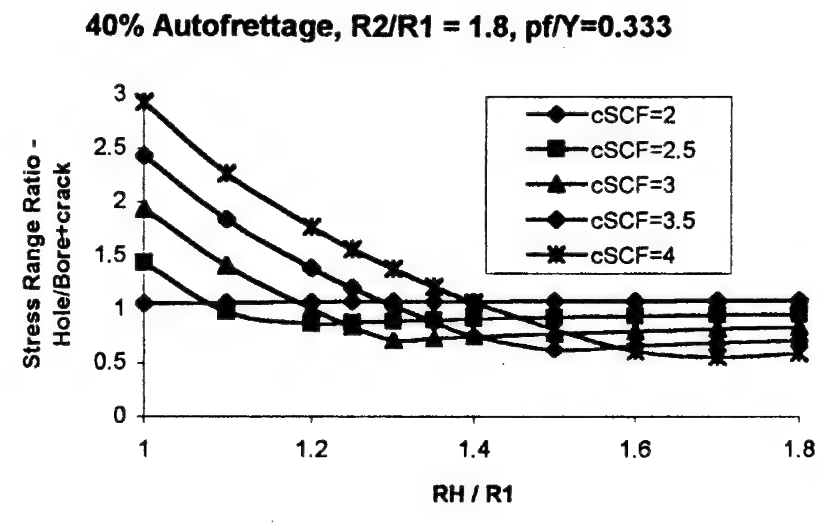
40% Autofrettage, R2/R1 = 1.8, pf/Y=0.333
Stress Range Ratio - Hole/Bore+crack
RH / R1
cSCF=2
cSCF=2.5
cSCF=3
cSCF=3.5
cSCF=4
0
0.5
1
1.5
2
2.5
3
1
1.2
1.4
1.6
1.8

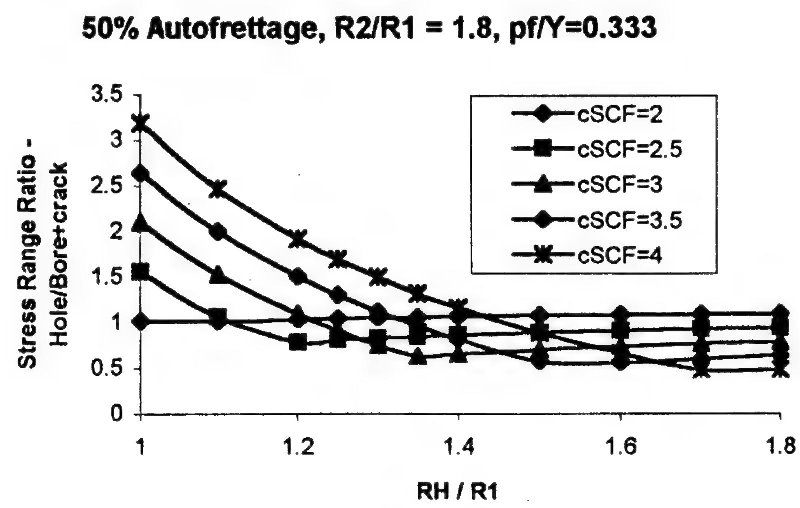
50% Autofrettage, R2/R1 = 1.8, pf/Y=0.333
Stress Range Ratio - Hole/Bore+crack
RH / R1
cSCF=2
cSCF=2.5
cSCF=3
cSCF=3.5
cSCF=4
0
0.5
1
1.5
2
2.5
3
3.5
1
1.2
1.4
1.6
1.8

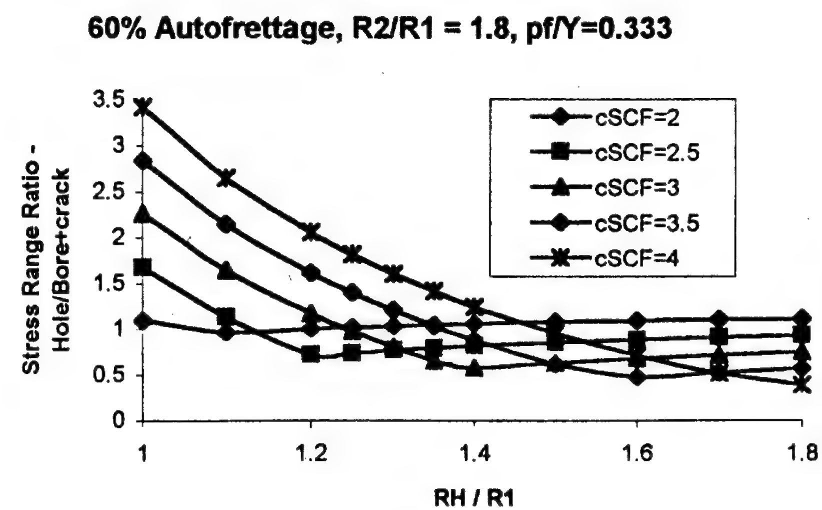
60% Autofrettage, R2/R1 = 1.8, pf/Y=0.333
Stress Range Ratio - Hole/Bore+crack
RH / R1
cSCF=2
cSCF=2.5
cSCF=3
cSCF=3.5
cSCF=4
0
0.5
1
1.5
2
2.5
3
3.5
1
1.2
1.4
1.6
1.8

70% Autofrettage, R2/R1 = 1.8, pf/Y=0.333

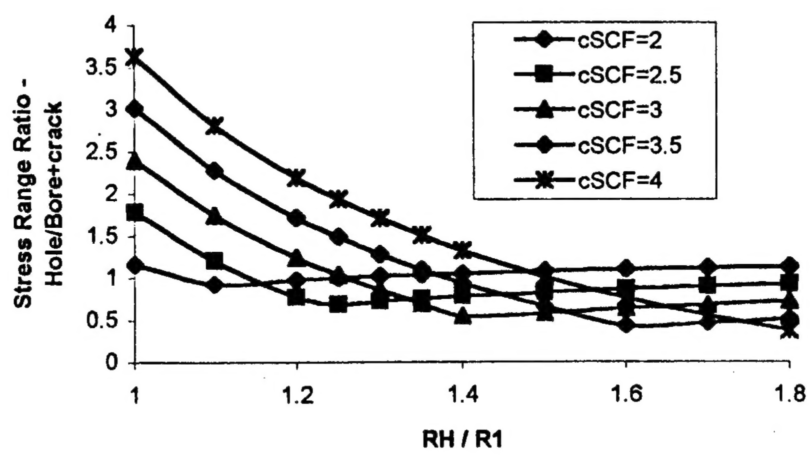

80% Autofrettage, R2/R1 = 1.8, pf/Y=0.333

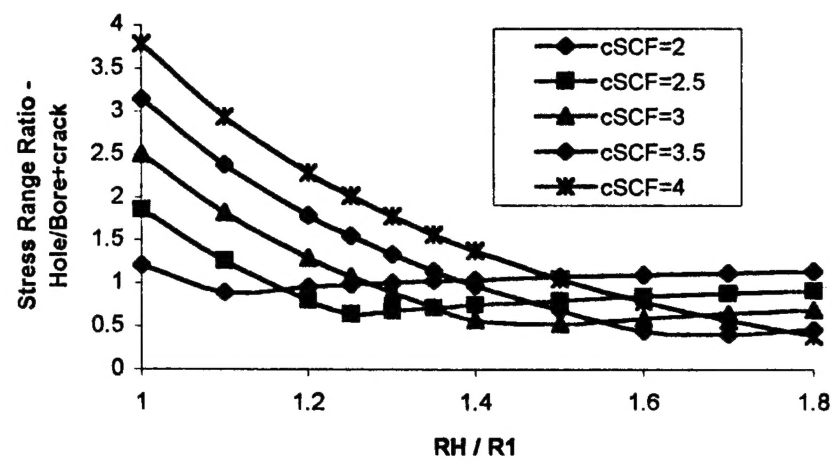

60% Autofrettage, R2/R1 = 1.8, pf/Y=0.333

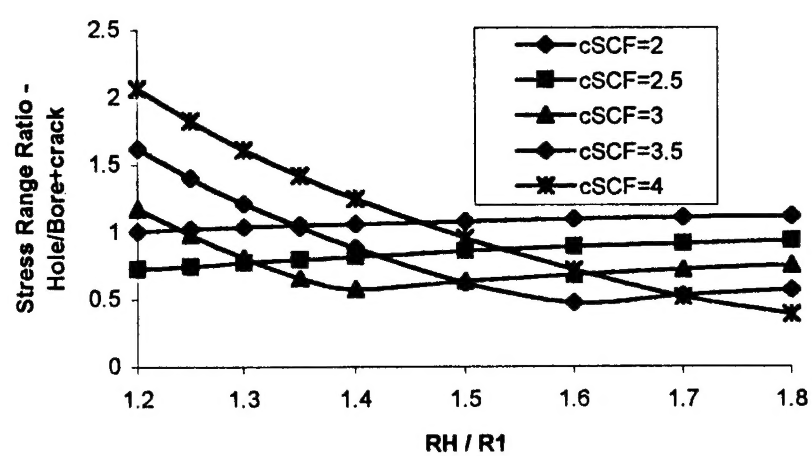

60% Autofrettage, R2/R1 = 1.8, pf/Y=0.333

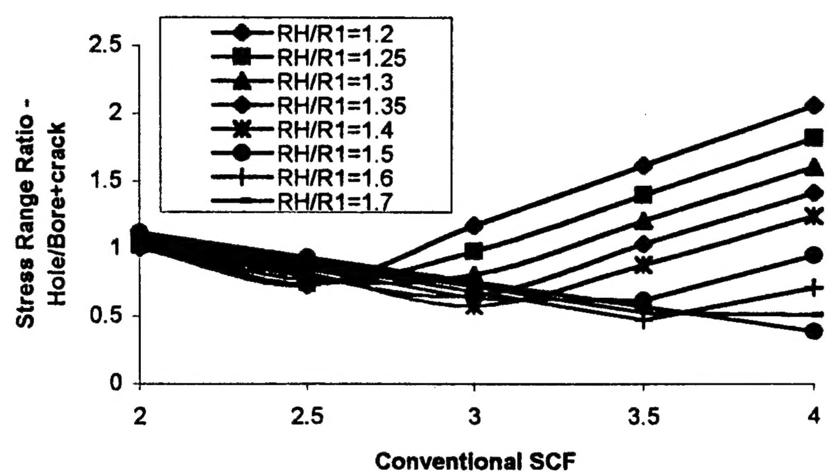

TECHNICAL REPORT INTERNAL DISTRIBUTION LIST

	NO. OF COPIES
CHIEF, DEVELOPMENT ENGINEERING DIVISION	
ATTN: AMSTA-AR-CCB-DA	1
-DB	1
-DC	1
-DD	1
-DE	1
CHIEF, ENGINEERING DIVISION	
ATTN: AMSTA-AR-CCB-E	1
-EA	1
-EB	1
-EC	1
CHIEF, TECHNOLOGY DIVISION	
ATTN: AMSTA-AR-CCB-T	2
-TA	1
-TB	1
-TC	1
TECHNICAL LIBRARY	
ATTN: AMSTA-AR-CCB-O	5
TECHNICAL PUBLICATIONS & EDITING SECTION	
ATTN: AMSTA-AR-CCB-O	3
OPERATIONS DIRECTORATE	
ATTN: SIOWV-ODP-P	1
DIRECTOR, PROCUREMENT & CONTRACTING DIRECTORATE	
ATTN: SIOWV-PP	1
DIRECTOR, PRODUCT ASSURANCE & TEST DIRECTORATE	
ATTN: SIOWV-QA	1

NOTE: PLEASE NOTIFY DIRECTOR, BENÉT LABORATORIES, ATTN: AMSTA-AR-CCB-O OF ADDRESS CHANGES.

TECHNICAL REPORT EXTERNAL DISTRIBUTION LIST

	NO. OF COPIES
ASST SEC OF THE ARMY	
RESEARCH AND DEVELOPMENT	
ATTN: DEPT FOR SCI AND TECH	1
THE PENTAGON	
WASHINGTON, D.C. 20310-0103	
DEFENSE TECHNICAL INFO CENTER	
ATTN: DTIC-OCP (ACQUISITIONS)	2
8725 JOHN J. KINGMAN ROAD	
STE 0944	
FT. BELVOIR, VA 22060-6218	
COMMANDER	
U.S. ARMY ARDEC	
ATTN: AMSTA-AR-AEE, BLDG. 3022	1
AMSTA-AR-AES, BLDG. 321	1
AMSTA-AR-AET-O, BLDG. 183	1
AMSTA-AR-FSA, BLDG. 354	1
AMSTA-AR-FSM-E	1
AMSTA-AR-FSS-D, BLDG. 94	1
AMSTA-AR-IMC, BLDG. 59	2
PICATINNY ARSENAL, NJ 07806-5000	
DIRECTOR	
U.S. ARMY RESEARCH LABORATORY	
ATTN: AMSRL-DD-T, BLDG. 305	1
ABERDEEN PROVING GROUND, MD 21005-5066	
DIRECTOR	
U.S. ARMY RESEARCH LABORATORY	
ATTN: AMSRL-WT-PD (DR. B. BURNS)	1
ABERDEEN PROVING GROUND, MD 21005-5066	
DIRECTOR	
U.S. MATERIEL SYSTEMS ANALYSIS ACTV	
ATTN: AMXSY-MP	1
ABERDEEN PROVING GROUND, MD 21005-5071	

	NO. OF COPIES
COMMANDER	
ROCK ISLAND ARSENAL	
ATTN: SMCRI-SEM	1
ROCK ISLAND, IL 61299-5001	
MIAC/CINDAS	
PURDUE UNIVERSITY	
2595 YEAGER ROAD	1
WEST LAFAYETTE, IN 47906-1398	
COMMANDER	
U.S. ARMY TANK-AUTMV R&D COMMAND	
ATTN: AMSTA-DDL (TECH LIBRARY)	1
WARREN, MI 48397-5000	
COMMANDER	
U.S. MILITARY ACADEMY	
ATTN: DEPARTMENT OF MECHANICS	1
WEST POINT, NY 10966-1792	
U.S. ARMY MISSILE COMMAND	
REDSTONE SCIENTIFIC INFO CENTER	2
ATTN: AMSMI-RD-CS-R/DOCUMENTS BLDG. 4484	
REDSTONE ARSENAL, AL 35898-5241	
COMMANDER	
U.S. ARMY FOREIGN SCI & TECH CENTER	
ATTN: DRXST-SD	1
220 7TH STREET, N.E.	
CHARLOTTESVILLE, VA 22901	
COMMANDER	
U.S. ARMY LABCOM, ISA	
ATTN: SLCIS-IM-TL	1
2800 POWER MILL ROAD	
ADELPHI, MD 20783-1145	

NOTE: PLEASE NOTIFY COMMANDER, ARMAMENT RESEARCH, DEVELOPMENT, AND ENGINEERING CENTER, BENÉT LABORATORIES, CCAC, U.S. ARMY TANK-AUTOMOTIVE AND ARMAMENTS COMMAND, AMSTA-AR-CCB-O, WATERVLIET, NY 12189-4050 OF ADDRESS CHANGES.

TECHNICAL REPORT EXTERNAL DISTRIBUTION LIST (CONT'D)

	NO. OF COPIES
COMMANDER U.S. ARMY RESEARCH OFFICE ATTN: CHIEF, IPO P.O. BOX 12211 RESEARCH TRIANGLE PARK, NC 27709-2211	1
DIRECTOR U.S. NAVAL RESEARCH LABORATORY ATTN: MATERIALS SCI & TECH DIV WASHINGTON, D.C. 20375	1
WRIGHT LABORATORY ARMAMENT DIRECTORATE ATTN: WL/MNM EGLIN AFB, FL 32542-6810	1
WRIGHT LABORATORY ARMAMENT DIRECTORATE ATTN: WL/MNMF EGLIN AFB, FL 32542-6810	1

NOTE: PLEASE NOTIFY COMMANDER, ARMAMENT RESEARCH, DEVELOPMENT, AND ENGINEERING CENTER, BENÉT LABORATORIES, CCAC, U.S. ARMY TANK-AUTOMOTIVE AND ARMAMENTS COMMAND, AMSTA-AR-CCB-O, WATERVLIET, NY 12189-4050 OF ADDRESS CHANGES.